NEURAL VARIABILITY, INFORMATION ENCODING, AND NOISE CORRELATIONS IN THE MOUSE VESTIBULAR NUCLEI

by
Aamna Lawrence

A thesis submitted to Johns Hopkins University in conformity with the requirements for the degree of Master of Science in Engineering

Baltimore, Maryland
August 2021

Abstract

In primates, regular semicircular canal afferents encode more average information about the stimuli across the behaviorally relevant frequencies ranging from 0 to 20 Hz compared to their irregular counterparts (Sadeghi et al., 2007a, b). At the next stage of vestibular stimuli processing, the vestibular-only (VO) neurons in the vestibular nuclei (VN), which contribute to posture control and self-motion perception, show even lower information transmission capabilities due to the higher variability in their responses when compared to even irregular afferent neurons (Massot et al., 2011). It has been suggested that the high neuronal variability of VO neurons is beneficial for the encoding of highly transient movement information. Indeed, recent studies have shown that these neurons use precise spike timing in millisecond order to encode highly dynamic stimuli (Jamali et al., 2016).

The mouse has become an increasingly popular animal model in neuroscience research. Single unit recordings have shown that mice VO neurons show similar responses as the primates for low frequency sinusoidal rotations but have lower sensitivities (Beraneck and Cullen, 2007). However, neither their information coding nor response dynamics have been studied over the frequency range of natural head movements. I hypothesized that the high neuronal variability and lower sensitivities of mouse VO neurons would decrease their overall information capacity relative to monkey VO neurons. To test this proposal, I used the neuropixel probes to record the

activity of VO neurons in the medial VN by subjecting the mice to a 1) broadband noise perturbation from 0 to 20 Hz, and 2) sinusoidal stimuli at 0.5, 1, and 2 Hz.

As seen in monkeys, the mice VO neurons in had lower coding fractions and higher gain and phase than monkey afferent neurons. Interestingly, the results showed that the mouse VO neurons had similar mutual information density and coding fractions across the frequency band of 0 to 20 Hz as primates. Population coding was also investigated where low pairwise noise correlations between the mouse VO neurons that were comparable to primates were observed. Thus, the study had important implications in understanding the sensory processing and neural circuitry of the mouse vestibular pathways.

Primary reader/advisor: Dr. Kathleen Cullen

Secondary readers: Dr. Kechen Zhang, Dr. Vikram Chib

Acknowledgements

This research investigation was conducted at the Center for Hearing and Balance in the Department of Biomedical Engineering and was funded by grants from the National Institute of Health.

First and foremost, I would like to thank my advisor, Dr. Kathleen Cullen for being motivating, patient, and keen on explaining the nuts and bolts of every aspect of the research work that I feel like a privileged student. She sparked my interest in neuroscientific research and I would continue to pursue the same in the future.

I would also like to thank Vanessa Chang for helping me in all the electrophysiological recordings and providing unique insights in all the brain-storming sessions we had regarding experimental protocol design and data analysis. Additionally, the help and feedback I received from all the members of the Cullen Lab, especially Omid Zobeiri, Yvette Tan, Olivia Leavitt, and Oliver Stanley, is highly appreciated. My parents also deserve special gratitude for encouraging me during my research work.

Thank you all so very much.

Aamna Lawrence

Table Of Contents

Abstract..... ii

Acknowledgements..... iv

List Of Figures..... viii

1. Chapter 1..... 1

1.1 General introduction..... 1

1.2 The peripheral vestibular system 3

1.2.1 Otolith organs:..... 4

1.2.2 Semicircular canals:..... 4

1.3 The central vestibular system..... 5

1.4. Stimuli processing in the VN 7

1.4.1 VO neurons:..... 7

1.4.2 Position-Vestibular-Pause (PVP) neurons:..... 8

1.4.3 Eye-head (EH) neurons:..... 8

1.5 Dual encoding strategy by vestibular afferents..... 9

1.5.1 Rate codes:..... 10

1.5.1.1 Linear dynamic models:..... 10

1.5.1.2 Non-linear models:..... 11

1.5.2. Temporal code: 12

1.5.2.1 Victor-Purpura metric:..... 13

1.5.2.2 van Rossum spike distance metric: 13

1.5.3. Quantification of information transmission: 13

1.6 Neuronal encoding in the central vestibular neurons..... 16

1.7 Neuronal correlations and population encoding..... 17

1.8. Optimal coding 19
1.9 Summary of the thesis goals 20
2. Chapter 2 21
2.1 Introduction 21
2.2 Materials and Methods 23
2.2.1 Surgical setup for VO neuron recording 24
2.2.2 Recording setup for VO neuron recording 26
2.2.3 Data acquisition 29
2.2.4 Marking lesions 30
2.2.5 Single-unit data analysis 30
2.2.5.1 Spike sorting 30
2.2.5.2 Baseline activity analysis of VO neurons 31
2.2.5.3 VO cell tuning 32
2.2.5.4 Estimation of MI and CF 32
2.2.5.5 Computation of noise correlations between VO neuron pairs 33
2.3 Results 34
2.3.1 Spontaneous activity of VO neurons 36
2.3.2 VO cell responses to sinusoidal head movements 38
2.3.3 Information transmission by mice VO neurons 39
2.3.4 Noise correlations between mouse VO neuron pairs 44
2.4 Discussion 48
2.4.1 Summary of the results 48
2.4.2 Comparable MI and CFs between mouse and monkey VO neurons 48
2.4.3 Anatomical influence of the VN on low noise correlation between VO neurons 50
2.5 Conclusion 51
3. Chapter 3 52
3.1 General discussion 52
3.1.1 Implications for the vestibular pathways mediating posture and self-motion perception 53

3.1.2 VN neurons contribute to the head direction network for spatial navigation 55
3.1.3 Consequences of low noise correlations on vestibular stimuli decoding..... 56
3.2 Concluding remarks 58
References ……59

List Of Figures

1.1 The peripheral vestibular system 6

1.2 The vestibular nuclei and its connections to other brain areas..... 7

1.3 Response of monkey horizontal canal irregular afferents to rotations of <500 deg/s..... 12

1.4 Schematic representation for the computation of the reconstructed stimuli from the spike train of the neuron..... 14

2.1 A 3D-rendered neuropixel probe holder for performing acute recordings..... 25

2.2 Experimental setup and stimuli used..... 27

2.3 Behavioral paradigms for dissociating eye and head movement sensitivity in the vestibular nuclei cells..... 28

2.4 Illustration of the ability of the neuropixel probe to record the simultaneous activity of many neurons in the medial vestibular nuclei responding to sinusoidal stimuli..... 29

2.5 Histological evaluation for confirming the location of the target recording site..... 30

2.6 Static firing properties of the mouse vestibular-only neurons..... 36

2.7 Comparison of the resting discharge and CV* of mouse vestibular-only (VO) neurons with their afferents and monkey VO neurons..... 38

2.8 Firing characteristics of mouse vestibular-only cells during sinusoidal head movements.... 39

2.9 Bode plot comparisons between mouse afferents, mouse vestibular-only (VO) and monkey VO neurons..... 40

2.10 Reconstruction of the stimuli for an example mouse vestibular-only neuron..... 42

2.11 Mutual information density and comparison of the coding fractions between mouse and monkey vestibular-only neurons..... 44

2.12 Noise correlation between mouse vestibular-only neurons..... 46

2.13 Relationship between correlated variability (CV) and noise correlation between the

pairs of vestibular-only neurons recorded simultaneously using neuropixel probes at 0.5 Hz sinusoidal stimulation……. 47

Chapter 1

1.1 General introduction

The vestibular system gives us our sense of head motion. Located in the inner ear, it senses head movement along the six axes, of which three are rotational, and the other three are translational. The information from the periphery is transmitted to the vestibular nuclei (VN) in the brainstem via the eighth cranial nerve comprising of the vestibular afferents, which constitute two parallel streams for transmitting low and high-frequency stimuli information (Jamali et al., 2016). Besides the vestibular input, the VN also receives cerebellar, oculomotor, cortical and neck proprioceptive inputs, thus acting as a site of multimodal integration. It also sends information to higher brain centers for spatial orientation and self-motion perception, eye muscles for stabilizing gaze, and the spinal cord for maintaining posture, thereby making the study of the sensory processing in the VN critical (Cullen, 2012).

In neuroscience, mice have become an invaluable animal model to study due to their comprehensively studied genetics and the availability of a wide variety of mutant strains. Additionally, they are amenable to the use of the latest technologies like optogenetics and neuropixel probes. Thus, they serve as good models to study neuronal encoding in the VN. However, so far, only a few major studies in non-human primates (NHPs) (Massot et al., 2011;

Jamali et al., 2016; Mitchell et al., 2018) have examined stimuli encoding in the central VN neurons, specifically the vestibular-only (VO) neurons. VO neurons are critical for mediating vestibulospinal reflexes to maintain balance and posture and show striking response similarities in mice and NHPs during passively applied low-frequency artificial stimuli (<=2Hz) (Goldberg, 2012; Beraneck and Cullen, 2007). Nevertheless, due to the difference in mice's physical anatomy and locomoting behaviour, it is reasonable to assume that the vestibular stimuli experienced by them are different from the NHPs, which could impact their central processing (Jamali et al., 2017).

It has already been shown that the mouse vestibular afferents show lower rotational sensitivities to head motion as compared to NHPs, reducing the amount of stimulus information they encode and pass on to the VN (compare Sadeghi et al., 2007a and Lasker et al., 2008). Furthermore, Beraneck and Cullen (2007) have shown similar resting variability but lower gains in the responses of mouse versus monkey VO neurons. Thus, it can be hypothesized that the mouse VO neurons transmit less information about the vestibular stimuli to the downstream areas for generating vestibulospinal reflexes and self-motion perception. However, to date, studies on mice models have never tested vestibular stimuli frequencies up to 20 Hz present during natural head movements. Thus, the central goal of this thesis was to investigate the information transmitted by the mouse VO neurons during a broadband noise perturbation containing the behaviorally relevant frequencies. In addition to the above, this study also investigated the presence of neuronal correlations between the VO neurons and compared them to the results obtained in NHP studies.

Accordingly, in this research study, single unit recordings were performed using 960-channel neuropixel probes, which have the unique advantage of capturing the simultaneous activity of many neurons along with providing high spatial and temporal resolution. Chapter 2 of the thesis is devoted to the analysis of the mouse VO neuron responses to passively-applied sinusoidal and broadband noise stimuli and their comparison with monkeys. Moreover, pairs of neurons were examined for the existence of any inter-neuronal correlations between them. The implications of the results on vestibular processing and higher-order functions in mice are discussed in Chapter 3.

In order to provide a more rigorous background of my study, in this introductory chapter, I will first provide a general overview of the peripheral and the central vestibular system. I would then discuss the different cell types in the VN of mice and monkeys, the dual stimuli encoding strategies used by the afferents, and its implications on the central vestibular neurons. More specifically, I would discuss rate code and temporal codes along with the models and metrics used in research to study them. Population encoding would be discussed next, where the different types of correlations between the neurons would be considered, followed by a review of optimized encoding in the VN.

1.2 The peripheral vestibular system

The vestibular system, considered the phylogenetically oldest sensory system, has sensory organs located in the petrous part of the temporal bone found in the inner ear (see Fig 1.1). The semicircular canals and the otoliths constitute the two types of sensors present in the

vestibular labyrinth. Mechanical deflections in the sensors lead to depolarization and repolarization of the hair cells which excite or inhibit the vestibular afferents innervating them. The two types of sensors are described below.

1.2.1 Otolith organs: The otolith organs are constituted by the utricle and saccule which sense linear acceleration along the three axes of translational motion and the direction and magnitude of gravity. The cilia of the hair cells found on their sensory epithelium are embedded in a gelatinous matrix topped with calcium carbonate crystals (otoconia). The inertia of the crystals bends the cilia of the hair cells during linear acceleration, thereby exciting or inhibiting them.

1.2.2 Semicircular canals: The three orthogonal semicircular canals, namely, the horizontal canal (HC), inferior/posterior canal (PC), and superior canal (SC), sense angular acceleration along the yaw, pitch and roll axes. The semicircular canals contain a viscous fluid and is interrupted by an ampulla containing the hair cells inside a water-tight and elastic cupula. When the head accelerates in the above-mentioned angular axes, the viscosity of the fluid in the semicircular canals bends the cupula, thereby depolarizing or hyperpolarizing the hair cells. While the canals sense head acceleration, the vestibular sensory afferents, synapsing with the hair cells, carry head velocity information. This integration of head acceleration is due to the tiny diameter of the semicircular canals and the inertia of the fluid.

The hair cells in both the sensory organs are of two types, namely, type I and type II. Type I hair cells are flask shaped and found only in amniotes. They contain larger amounts of potassium channels activated by calcium and thus show low detection thresholds for high-frequency head

movements. On the other hand, type II hair cells are cylindrical and phylogenetically older and are present in both amniotes and non-amniotes (Eatock and Songer, 2011). The stimulus information from the peripheral vestibular system is carried by the regular and irregular afferents which synapse with the type II and type I hair cells, respectively.

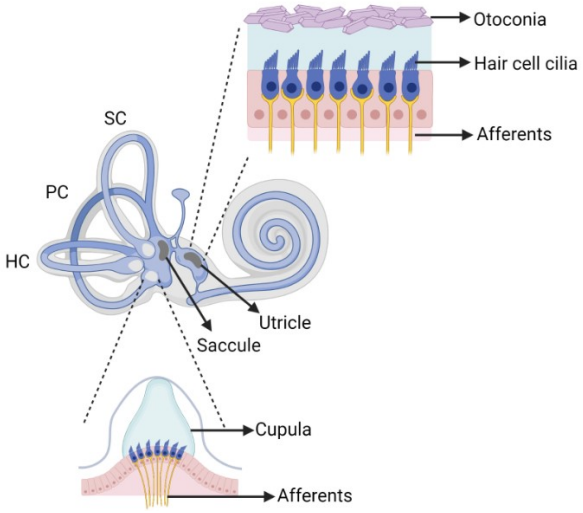

Fig. 1.1: The peripheral vestibular system. Head acceleration is detected along the angular axes by the horizontal (HC), posterior (PC) and superior canals (SC) due to the deflection of the cupula which houses the stereocilia of the hair cells. The utricle and saccule detect linear acceleration by the shear movement of the otoconial mass which bends the hair cell cilia.

1.3 The central vestibular system

Afferent fibers projecting from the semicircular canals and otolith organs are not typically segregated in the VN, however, the vestibular complex can be roughly divided into four major subdivisions, namely the medial VN (MVN), lateral VN (LVN), superior VN (SVN), and the inferior VN (IVN) (Goldberg, 2012).

First, the MVN, found below the floor of the fourth ventricle, makes the largest subdivision of the VN and is also called the principal VN. While the vestibulo-ocular cells are concentrated in the rostral third of the MVN, the vestibulospinal cells are found in the caudal region. It mostly gets input from the horizontal semicircular canals and would thus be the target recording site in the study. Second, the LVN is bound laterally by the inferior cerebellar peduncle and dorsally by the y-group cells which form a dorsal cap on it. Utricular and saccular afferents terminate at the LVN. Third, the SVN is located between the superior cerebellar peduncle and LVN and is the most easily recognizable VN. It receives input from the vertical semicircular canals. Finally, the IVN is located medial to the inferior cerebellar peduncle and is a caudal extension of LVN. It is characterized by rostro-caudal bundles running along its length, originating from the cerebellum or inferior olive, and receiving major input from the utricular afferents (Goldberg, 2012).

Information from the VN is conveyed to other brain regions as well, and in most cases, the connections are bidirectional (see Fig. 1.2). Direct projections from the VN go to the oculomotor nuclei to ensure stable images on the retina during head motion. Projections also go to the spinal cord for head stabilization with postural changes. Moreover, reciprocal connections with the cerebellum enable the computation of an internal estimation of the body's motion in space, and connections to the cerebral cortex via the thalamus bring about self-motion and spatial perception. It also sends secondary projections to the limbic system for more specific spatial information encoding (Cullen, 2012).

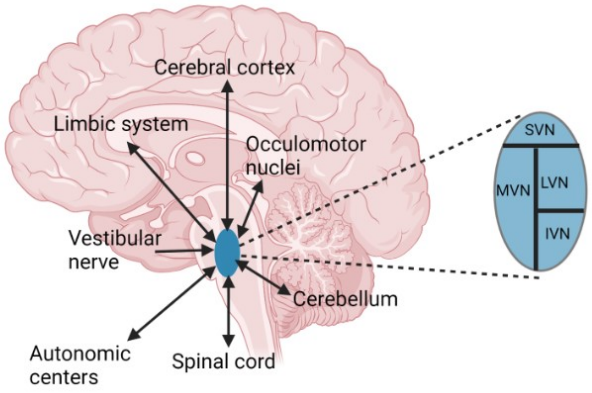

Fig. 1.2: The vestibular nuclei (VN) and its connections to other brain areas. It comprises of 4 major subdivisions namely the superior (SVN), medial (MVN), lateral (LVN), and inferior VN (IVN). Moreover, it receives input from the vestibular nerve afferents and is interconnected with the cerebral cortex, limbic system, oculomotor nuclei, autonomic centers, spinal cord and cerebellum which mediate reflexive eye movements, postural control, and self-motion and spatial orientation perception.

1.4. Stimuli processing in the VN

Three classes of neurons have been identified in the VN of primates based on their activity in response to vestibular stimulation and eye movements (Goldberg, 2012). VN neurons stimulated by the horizontal canals have been well-characterized in alert animals. During yaw rotations, these neurons are further classified into type I and type II neurons. Type I neurons increase their discharge when the head movement is ipsilateral to the recording site while the type II neurons increase their activity during contralaterally directed head movements.

1.4.1 VO neurons: VO neurons are also called the non-eye movement-related neurons, which respond neither to fixation nor smooth pursuit. They receive monosynaptic inputs from the vestibular nerve and do not project to the extraocular motor neurons. Instead, they send

projections to the spinal cord and are reversibly interconnected with the cerebellum. Moreover, they reduce their sensitivity to head motion during active or self-generated movements, thereby suppressing unwanted spinal reflexes during voluntary motion (reviewed in Cullen et al., 2011). Consequently, they are critical for vestibulospinal and vestibulocollic reflexes and the maintenance of posture. They also contribute towards self-motion and spatial orientation perception. Thus, understanding their encoding of the vestibular stimuli as single units and as a population would be the focus of this study.

1.4.2 Position-Vestibular-Pause (PVP) neurons: The type I PVP neurons respond to ipsilateral head movement, contralateral eye position, and pause during ipsilaterally directed saccades and quick phases of vestibular nystagmus. The opposite is true for type II PVP neurons. PVP neurons are found primarily in the rostral MVN and send direct excitatory projections to the extraocular motor neurons, namely in the contralateral abducens nucleus or ipsilateral medial rectus subdivision of the oculomotor nucleus. While the type I PVP neurons form a major part of the three-neuron arc for mediating horizontal vestibulo-ocular reflex, type II PVP neurons are involved in generating translational vestibulo-ocular reflex and pausing the activity of type I PVP neurons via inhibitory commissural pathways during ipsilateral saccades.

1.4.3 Eye-head (EH) neurons: EH neurons increase their discharge to ipsilateral eye movements during smooth pursuit, head movements during vestibulo-ocular reflex cancellation (where the eye stays stationary in the orbit), and eye position during fixation, thereby encoding gaze. These neurons are found in the rostral MVN and rostroventral LVN and receive inhibitory input from

the flocculus and excitatory inputs from the ipsilateral and contralateral vestibular nerve. They bring about smooth-pursuit movements and vestibulocollic reflex by projecting to the ipsilateral extraocular motor neurons and neck motor neurons, respectively.

To date, cells in the VN of the alert mouse have primarily been classified as eye-sensitive (ES) and VO neurons. The VO cells in mice share similar response characteristics with monkeys (Beraneck and Cullen, 2007). This is because studies have shown that the afferents projecting to the central vestibular neurons have similar resting discharges and dependence of response dynamics on discharge irregularity in mice and monkeys (Lasker et al., 2008; Sadeghi et al., 2007a).

1.5 Dual encoding strategy by vestibular afferents

In mammals, the vestibular nerve afferents innervating the vestibular receptors present in the semicircular canals and otoliths are grouped into two classes, namely, regular and irregular, based on the consistency of the spacing between the spontaneous action potentials, also referred to as the inter-spike interval (ISI). The difference in their responses of the two afferent classes was attributed to the variation in the potassium ion conductance in their membranes (Smith and Goldberg, 1986). The response variability in the afferents has been quantified using the coefficient of variance (CV) which is computed by taking the ratio of the standard deviation and mean of the ISI. In monkeys, irregular afferents have a normalized CV ≥0.1, whereas regular afferents have a normalized CV < 0.1 (Schneider et al., 2015).

Regular and irregular afferents form two parallel information pathways for carrying low and high-frequency stimuli information using rate and temporal codes, respectively, to the central vestibular neurons (Jamali et al., 2016). For this study, I will primarily focus on work done previously on the monkey HC afferents.

1.5.1 Rate codes: One of the ways neurons encode a stimulus is by representing its attributes by the number of spikes in a time window whose length is determined by the stimulus timescale, and the precision of the spike timing is not critical. Several studies have previously established that the regular and the irregular vestibular afferents encode the head motion stimuli using rate codes where they carry detailed information of the entire time course of the stimuli by changing their firing rate (reviewed in Goldberg, 2012; Cullen, 2012; Cullen and Roy, 2004; Sadeghi et al., 2007a; Schneider et al., 2015; Sadeghi et al., 2007b). Linear and non-linear models have been implemented to estimate the firing rates in these neurons.

1.5.1.1 Linear dynamic models: Numerous studies have previously used linear systems to capture the input-output relationship between the low intensity head movement and the firing rate of the afferents and predict the firing rate response (reviewed in Goldberg, 2000; Cullen, 2004; Massot et al.,2012; Sadeghi et al., 2007a). Such models work when the neuronal output increases linearly with the input (homogeneity) and given two inputs, the output is the linear sum of outputs when the two inputs are applied separately (additivity).

In the studies mentioned above, the time-dependent estimated firing rate of the canal afferents during passive-whole body sinusoidal rotations has been computed using a linear model as:

$$r_{linear}(t) = r_0 + (H * s)(t),$$

where r_0 is the resting discharge, H is the canal transfer function convolved with $s(t)$, the head velocity stimuli. The transfer function $H(f)$, was given by

$$H(f) = \frac{P_{sr}(f)}{P_{ss}(f)},$$

where $P_{sr}(f)$ and $P_{ss}(f)$ represent the cross-spectrum between the neuronal response $r(t)$ and stimulus $s(t)$, and power spectrum of the stimulus, respectively.

1.5.1.2 Non-linear models: During naturalistic movements like jumping, climbing, and running, the head velocity of monkey and mice can go up to 1500 deg/s and 1300 deg/s, respectively (Carriot et al., 2017). In such instances, linear models fail to predict the firing rate responses since the neurons show non-linear behavior. In other words, during high amplitude head movements, the firing rate predicted by the linear models show cut-off in the off-direction (rectification) and a plateau at the maximum value in the on-direction (saturation).

Schneider et al. (2015) established a linear-non-linear cascade model to predict the firing rate of the afferents at highly dynamic behaviors which is given by:

$$r_{non-linear}(t) = T_{non-linear}\big((H * s)(t) + r_0\big),$$

where $T_{non-linear}$ is a non-linear sigmoidal function.

The model worked particularly well for predicting the neural responses of the irregular afferents (see Fig 1.3) since they show higher sensitivities to the stimuli as compared to the regular afferents, thereby suggesting that the irregular afferents play an important role in encoding naturalistic behaviors (Schneider et al., 2015).

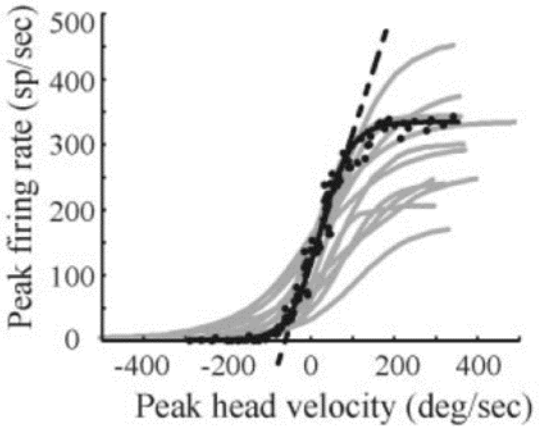

Fig. 1.3: Response of monkey horizontal canal irregular afferents to rotations of <500 deg/s (dashed and solid lines represent the firing rate predicted from a linear model and non-linear model, respectively) (Sadeghi et al., 2007a).

1.5.2. Temporal code: Neurons also encode the attributes of a stimuli by showing exact spike timing/phase locking within a time window A substantial study by Jamali et al. (2016) showed that instead of using rate code, irregular afferents in NHPs use precise spike timing in the order of milliseconds (~6 milliseconds) to capture stimuli information. Several metrics were used in the study to compute the similarity between the spike trains to repeated representations of the same stimuli.

1.5.2.1 Victor-Purpura metric: This cost-based metric computes the dissimilarity between two spike trains. In other words, it estimates the minimum cost for transforming one spike train into another using deletions and additions of spikes where one such operation counts for a cost of 1. The cost of shifting the spike by Δt is given by $q\Delta t$ where q (in units of s^{-1}) determines how spike timing and spike count affects the metric. For rate codes, q is taken as 0, however, high values of q are used when temporal codes are considered.

1.5.2.2 van Rossum spike distance metric: For computing this metric, each spike train is convolved with an exponential kernel having a time constant τ and is represented by:

$$f(t) = \sum_{i=1}^{M} H(t - t_i) e^{\frac{-(t-t_i)}{\tau}},$$

where, t_i is the timing of the spikes, M is the total number of spikes and $H(t)$ is the Heaviside step function $H(t) = 0$ for $t < 0$ and $H(t) = 1$ for $t \geq 0$. The distance between the spike trains $R_j(t)$ and $R_k(t)$ is computed as the Euclidean distance between their convolved spike trains with the kernel, $f_{R_j}(t)$ and $f_{R_k}(t)$, respectively:

$$D^2\left(f_{R_j}(t), f_{R_k}(t)\right)_\tau = \frac{1}{\tau}\int_0^\tau (f_{R_j} - f_{R_k})^2 dt.$$

The τ parameter measures how temporally sensitive the metric is and is given by $1/q$ from the Victor-Purpura metric.

1.5.3. Quantification of information transmission: While the linear and the non-linear models mentioned above help explain the neuronal responses, it is essential to assess the performance

of these models and quantify how well the stimuli characteristics are represented in their firing rates.

One of the quantification techniques is the computation of the coding fraction (CF). CF represents the fraction of the stimulus that can be accurately reconstructed from the spike train of a neuron and can range from 0 to 1 (Sadeghi et al., 2007b). Several studies have used stimuli reconstruction techniques by convolving the spike trains of the neurons with an optimal kernel (see Fig 1.4) and evaluated CFs as follows (Sadeghi et al., 2007b; Massot et al., 2011):

$$CF = 1 + \frac{\varepsilon}{\sigma_{stim}},$$

where ε is the root mean squared error between the actual ($s(t)$)and estimated ($s_{reconst}(t)$) stimulus waveform and σ_{stim} is the standard deviation of the stimulus.

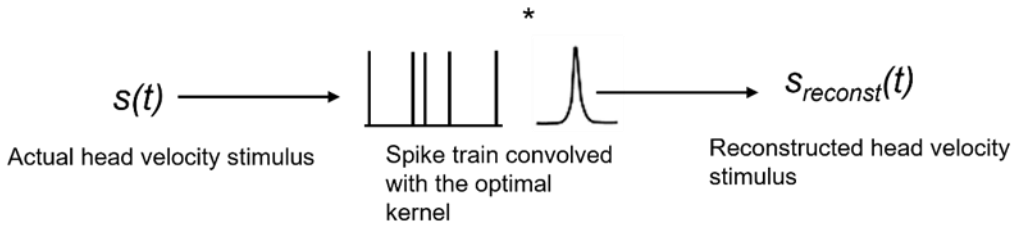

Fig. 1.4: Schematic representation for the computation of the reconstructed stimuli from the spike train of the neuron. The spike train of the neuron modulating to the head velocity stimulus was convolved with an optimal filter to generate the reconstructed head velocity signal (Sadeghi et al., 2007 a, b; Massot et al., 2011)

Another measure of the amount of information about the stimuli carried by the neuronal spike train if by computing the coherence. Coherence between the neuronal response and the

stimulus provides a lower bound on the amount of information that can be obtained from the former about the later by taking neural variability into account. Coherence and the mutual information (MI) shared between the neuronal response and stimuli can be represented as (Massot et al., 2011; Massot et al., 2012):

$$C(f) = \frac{|P_{sr}(f)|^2}{P_{ss}(f)P_{rr}(f)},$$

$$MI_{lower} = -log_2\big(1 - C(f)\big).$$

Here, $P_{rr}(f)$ represents the power spectrum of the response $r(t)$ and MI is calculated in bits per second per Hertz which can be normalized by dividing it with the mean firing rate. The signal-to-noise ratio (SNR) can be computed from the coherence as (Massot et al., 2012):

$$SNR(f) = \frac{C(f)}{1 - C(f)}.$$

It has previously been established that the vestibular system is adapted to the statistical structure of the naturalistic stimuli (Attneave, 1954; Laughlin, 1981; Barlow, 2001; Simoncelli and Olshausen, 2001). Since NHPs have different posture and locomoting behaviour as compared to rodents, the vestibular stimuli experienced by them varies significantly from the mice. NHPs have larger canal arc sizes and their vestibular canal afferents are 3-4 times more sensitive to head movement as compared to mice (i.e. compare Sadeghi et al., 2007a and Lasker et al., 2008). However, the variability in the responses of the canal afferents is the same across both the species (Lasker et al., 2008; Sadeghi et al., 2007a). Consequently, the information encoded by the

mouse canal afferents has a lower signal to noise ratio as compared to monkeys which would influence its central processing and was explored in this study.

1.6 Neuronal encoding in the central vestibular neurons

Like the vestibular afferents, the notion of rate coding in the central vestibular neurons prevailed in several previous research studies (reviewed in Cullen, 2012; Cullen and Roy 2004; Massot et al., 2011; Massot et al., 2012). Consequently, linear as well as linear-non-linear cascade models have been used to predict the firing rates of these neurons (Massot et al., 2012).

Besides showing static non-linearities like rectification and saturation, VO neurons have also been found to show boosting non-linearities (Massot et al., 2012). During boosting, VO neurons disobey the principle of superposition or additivity. In other words, when high and low frequency stimuli are presented together, the lower frequency is attenuated and the firing rate represents the higher frequency as if it was presented alone (Massot et al., 2012). This masking of the low frequency component of the stimulus enables the cells to respond to high intensity dynamic movements.

The breakthrough study by Jamali et al., (2016) in NHPs showed that not only irregular afferents, but also the VO neurons show temporal coding. According to the study, this type of encoding strategy enabled the VO neurons to capture highly dynamic stimuli in millisecond timescale to respond to unexpected transient vestibular stimuli like slipping on ice and generate vestibulospinal reflexes. Moreover, the precision in the spike timing led to synchronization in

their activity as a population to drive high-inertia reflexive movements and overcome perceptual threshold of self-motion (Jamali et al., 2016).

As discussed in the previous section, mouse irregular afferents have a lower SNR than NHPs which synapse with the VO neurons in the VN. Moreover, mouse VO neurons have been shown to have similar fluctuations in their resting discharge, but lower gains as compared to monkeys (Beraneck and Cullen, 2007). Therefore, it can be predicted that they encode less stimulus information in their spike trains than primates. Thus, this study explored how the low head motion information transmitted by the irregular afferents affected the central processing of the stimulus in the mouse VO neurons using broadband noise stimuli having natural head movement frequencies.

1.7 Neuronal correlations and population encoding

Neurons work as a democracy, where the population instead of individual neuronal activity drives behavior and perception. Population activity typically comprises of tuning to a behaviorally relevant stimuli along with noise (Averbeck et al., 2006). The noise arises due to the variable activity of a neuron to repeated presentations of the same stimuli. This neural variability makes population activity highly probabilistic and difficult to understand.

In the brain, correlations among the activity of the neurons can be of various types, namely, signal correlation, noise correlation, synchrony and long timescale correlation (Cohen and Kohn, 2011). Signal correlation is defined as the correlation between the mean activity of the neurons to a given stimuli and gives the of measure of the tuning of the neurons to a particular

stimulus. Noise correlation or spike time correlation is the correlation between the spike counts among the pairs of neurons for the same stimuli and in the same behavioral setting. Synchrony refers to the precise temporal alignment of spikes over small timescales of a few milliseconds to one second, whereas long timescale correlation is the correlation between a neuron whose response is measured in the future or past as compared to the other neuron. Understanding population coding not only improves our understanding of sensory processing but also allows us to infer brain connectivity and its architecture. Moreover, studying noise correlations in the VO neurons in the VN is critical because they receive direct synaptic input form the irregular afferents which contributes to their high variability.

The role of noise correlations on population coding is highly debated. On one hand if noise is uncorrelated and detrimental to information transmission then, as a population, the noise would cancel out. However, if the noise is correlated, it might carry important information about the stimuli (Averbeck et al., 2006). Correlated variability has been previously seen in sensory neurons in certain cortical areas like visual cortex of macaques which plays an important role in decision-making (Britten et al. 1996). In the nucleus prepositus of monkeys, synchrony has been reported between eye-sensitive neurons due to the common synaptic inputs received by the nearby pairs of neurons (Dale and Cullen, 2015).

Studies have shown that connexin-36 gap junctions are prevalent in the VN (Condorelli et al., 2000; Beraneck et al. 2009). Thus, it can be hypothesized that they might play a significant role in contributing towards noise correlations by promoting electronic coupling between the VO neurons in mice, thereby affecting population encoding. Noise correlations might also arise since

more than one afferent can innervate a single type II hair cells (Eatock et al., 1998) and a single afferent can synapse with multiple VO cells (Sato et al., 1989), and thus sending a common input to them. However, Liu et al. (2013) has reported negligible noise correlations between the VN neurons in monkeys.

To reach a more definitive answer, this study used neuropixel probes to record the simultaneous activity of several pairs of VO neurons across trials having the same stimuli to determine if the fluctuations in their neural activity were correlated.

1.8. Optimal coding

The natural statistics of the vestibular stimuli is unique since its power decreases gradually at lower frequencies (~<3 Hz) and more rapidly at higher frequencies (~>6Hz), thereby deviating from the power law (Carriot et al., 2014). To effectively encode the stimuli at frequencies as high as 20 Hz and maximize the transmission of information, the neurons of the VN in monkeys have been found to show temporal whitening where they maintain a constant power spectrum above 2 Hz (Mitchell., 2018). They not only increase the tuning to the stimulus at higher frequencies but also match the frequency spectrum of their neural variability with the tuning function. Such temporal whitening has been shown to occur in stages with some temporal decorrelation occurring at the level of the peripheral vestibular afferents (irregular afferents) and then the central vestibular neurons. Thus, more the variability, higher is the temporal whitening (Mackrous et al., 2020).

The temporal whitening shown by the VO neurons along with their precise spike timing and phase locking with the stimuli would lead to more synchronized population neuronal response at higher naturalistic frequencies which mediate vestibulospinal reflexes to overcome the inertia of the head-neck system (Mackrous et al., 2020). Thus, in this study, the presence of whitening in the responses of VO neurons was also investigated for the mouse model.

1.9 Summary of the thesis goals

The vestibular system is a well-studied sensory system with comprehensive characterized cells responding to a straightforward and easily described temporally-varying head motion stimuli (Cullen 2011). This makes it an ideal system for studying sensory stimuli processing.

The first aim of the thesis was to analyze the responses of the mouse VO neurons in the MVN to passively applied sinusoidal and broadband noise stimuli in the yaw axes. Information theory metrics namely, MI and CF were used for the first time to quantity the stimulus details encoded by the mouse VO neurons and compared with the NHPs.

As the second aim of my thesis, pairwise activity of several VO neurons recorded simultaneously using neuropixel probes were examined to compute the presence of any correlated variability between them. This evaluation provided valuable information about population coding and decoding of the stimulus by downstream areas.

In all, this thesis provided major insights about the vestibular stimuli processing at the lowest level of central processing in one of the most fundamental animal models in neuroscience, the mice, and drew comparisons with primate studies.

Chapter 2

2.1 Introduction

Understanding sensory processing is one of the primary goals of systems neuroscience. However, studying the transformation of sensory input for generating the correct behavior and perception is complicated since neurons show response variability to repeated presentations of the same stimuli, which increases from the peripheral to the central brain regions (Dean, 1981; Mainen and Sejnowski, 1995; Tolhurst et al., 1983; Gabbiani et al., 1996; Shadlen and Newsome, 1998; Softky and Koch, 1993).

The vestibular system is a highly well-characterized sensory system that senses our head motion in space and is necessary to make reflexive eye movements, maintain posture and balance, and perceive voluntary motion and spatial position. The peripheral vestibular afferents, namely the regular and the irregular afferents, carry head movement information to the vestibular nuclei (VN), the site of multimodal integration and early vestibular stimuli processing (Cullen, 2012). The vestibular-only (VO) neurons found in the VN constitute an important class of neurons since they are involved in the generation of the vestibulospinal reflexes (reviewed in Cullen, 2019). Additionally, they are involved in higher-order functions like perception of self-motion and orientation in space via their projections to thalamocortical pathways.

Previous studies by Massot et al. (2011) and Sadeghi et al. (2007b) in non-human primates (NHPs) showed that monkey VO neurons display higher gains than the regular and irregular afferents. However, since they also displayed higher variability in their baseline firing rate, they conveyed a low amount of information about the stimulus to the higher brain areas as compared to their afferent class. A subsequent study by Jamali et al. (2016) further established that the precise patterning of action potentials in the responses of VO neurons allowed them to encode the unique and detailed time course of highly dynamic and transient stimuli on the order of milliseconds when it was presented multiple times. This coding strategy, termed temporal coding (Theunissen and Miller, 1995; Abbott and Dayan, 2001; Aldworth et al., 2011), is also employed by irregular but not regular afferents (Jamali et al., 2016).

Over the past decade, the mouse has become one of the most extensively studied animal models in neuroscience. Similar to monkeys, the VN of mice has been characterized using single unit neurophysiological recording experiments. To date, it has been shown that the mouse VN comprises of VO neurons which have similar firing statistics as monkeys despite having lower sensitivity to head movement for frequencies up to 2 Hz (Beraneck and Cullen, 2007; Massot et al., 2011). Thus, it can be hypothesized that the stimulus information conveyed by the mouse VO neurons would be worse than primates. Moreover, this hypothesis would hold for higher frequencies encountered during natural head movements. However, studies in mice have not yet explored the coding of vestibular stimuli in the behaviourally relevant frequency range of 0 to 20 Hz. Further, no study has quantified information coding by mouse VO neurons and/or investigated whether these neurons use temporal coding to transmit vestibular information.

Accordingly, in my thesis research study, I recorded from mouse VO neurons during stimulation with vestibular stimuli spanning the behaviourally relevant frequency range of 0 to 20 Hz. Specifically, neuronal recordings were performed using high-density neuropixel probes, which provide a good resolution of many single unit activities recorded simultaneously, while mice were subjected to a sinusoidal (0.5, 1, 2 Hz) and broadband noise stimulus (0 to 20 Hz). Neuronal resting and dynamic firing modulation were quantified and then compared with published values for monkey VO neurons. I also estimated mutual information (MI) density and the coding fraction (CF) of the recorded mouse VO neurons in response to broadband noise stimulation. Overall, I found that the information transmission capacities of mouse and monkey VO neurons were comparable. Finally, the impact of noise correlation on population coding was studied among pairs of mice VO neurons recorded simultaneously with the neuropixel probes. Taken together, the results of my thesis provide the first reports of (i) the application of information theory to the encoding of behaviourally relevant vestibular stimuli and (ii) the inter-neuronal variability of VO neurons by using the neuropixel probes in the mouse model.

2.2 Materials and Methods

Two male C-57bl6 (28-30g) adult mice (5 months) were used in the study. A total of 18 well-isolated VO cells were examined, of which 15 were recorded on the turntable and 3 on the hexapod. All the procedures were approved by the Johns Hopkins University Animal Care and Use facility which is strictly regulated by the Animal Welfare Act regulations and Public Health

Service (PHS) Policy and accredited by the private Association for the Assessment and Accreditation of Laboratory Animal Care (AAALAC) International.

2.2.1 Surgical setup for VO neuron recording

Mice were sedated with an intraperitoneal shot of ketamine (10-1mg/g), atropine (5.10−4 mg/g), acepromazine maleate (2.5.10−2mg/g), xylazine (10−1mg/g), and sterile saline. An analgesic injection of bupivacaine (2ml) was administered subcutaneously before the surgery. A brief anterior-posterior incision was made to expose the skull surface and the pericranium was removed. The skull was wiped with sterile saline and primed using Optibond. Hydrogen peroxide was spread on the skull to make the bregma and lambda visible. The mouse brain atlas was used to find the stereotaxic coordinates for drilling the skull to perform single-unit recordings in the VN and a craniotomy of 2mm diameter was performed. A custom-made 3D-printed neuropixel probe holder, which enabled acute recordings and movement of the probe by 1 mm in the x-y plane, was designed (see Fig 2.1). The probe holder and the custom-made aluminum head post were fixed to the skull using dental cement.

Additionally, a magnetic sensor was secured on the anterior portion of the skull above the left eye, which was implanted with a magnetic eye sensor (Payne and Raymond, 2017) to track eye movements. The dental cement was cured with brief exposure to UV light. Care was taken during the surgical procedure to avoid hypothermia or dehydration. The scalp incision was sutured using VetBond, and an antibiotic ointment (Thiocelline) was applied on the scalp to

prevent infection. After the surgery, the animals were kept in separate cages and monitored closely for 48 hours.

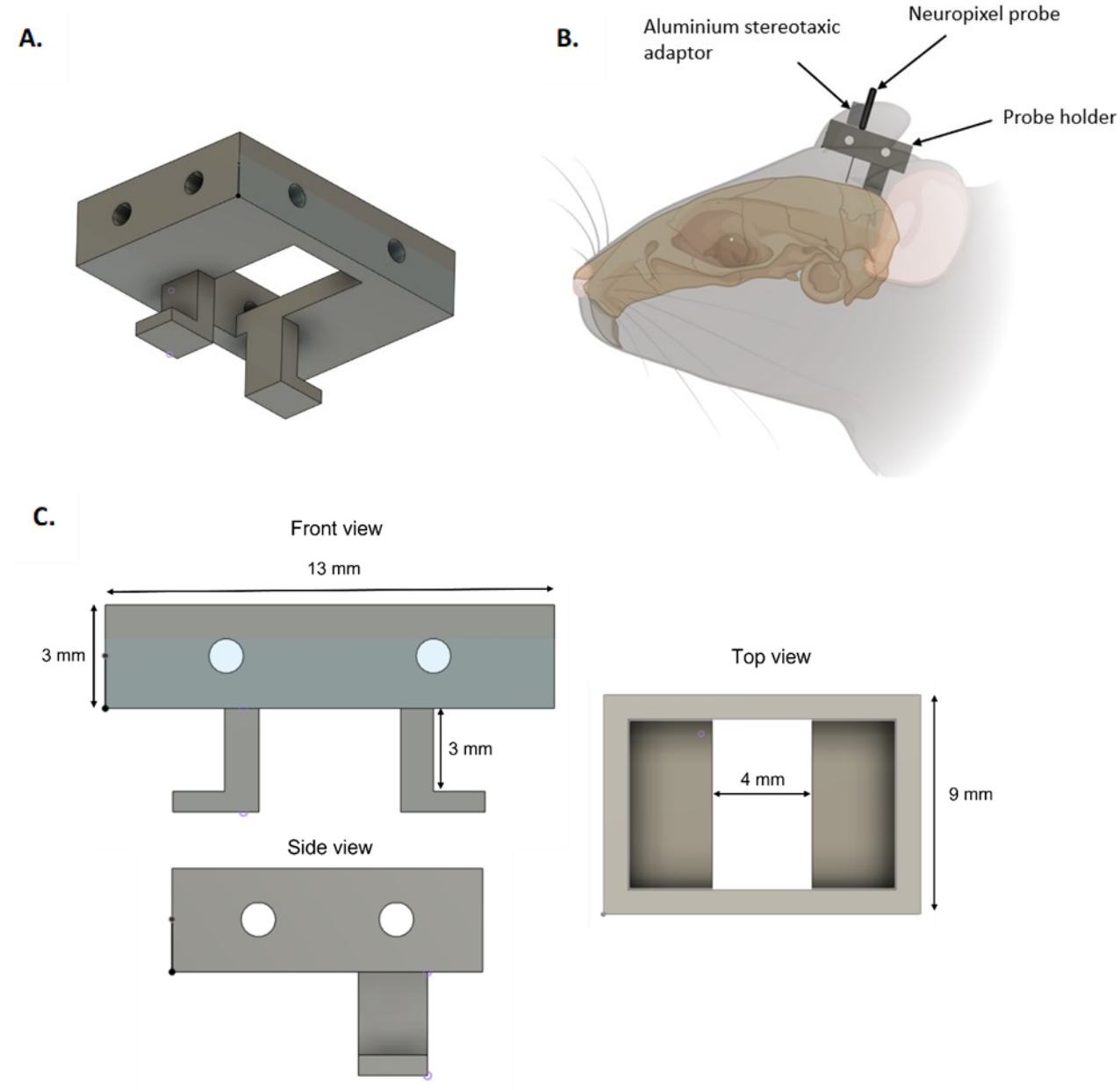

Fig. 2.1: A 3D-rendered neuropixel probe holder for performing acute recordings. A. The neuropixel probe holder designed using the AutoDesk Fusion 360 software. B. Placement of the probe holder on the mouse skull. The neuropixel probe was attached to the stereotaxic aluminium adaptor and the assembly was secured on the probe holder using screws. Dental cement was used to fix the probe holder on the mouse skull C. Different views of the probe holder with its dimensions

2.2.2 Recording setup for VO neuron recording

Two recording setups were used in the study. The first recording setup comprised of a turntable (see Fig 2.2). The mouse was placed head-fixed in a mouse tube mounted on a turntable. The vestibulo-ocular reflex (VOR) paradigm was performed by moving the turntable at 40 deg/s for different frequencies, namely, 0.5, 1, 2 Hz. In order to make sure that the cells were not sensitive to eye movement, the static eye position (SEP) and optokinetic reflex (OKR) paradigms were also performed in addition to the VOR paradigm (see Fig 2.3). During the SEP paradigm, the eye was moved to different eccentric positions in the orbit (~20 deg) by only moving the turntable. In contrast, during the OKR paradigm, the turntable was kept stationary and the visual surround was moved at an angular velocity of 10 deg/s. Each paradigm lasted for 15-20 seconds.

The second recording setup consisted of a hexapod having six degrees of freedom (see Fig 2.2B). The mouse was placed head-fixed in a tube fixed on the hexapod platform. Broadband noise stimulus with frequencies from 0 to 20 Hz was played in the yaw (horizontal) plane for 40 seconds.

A.

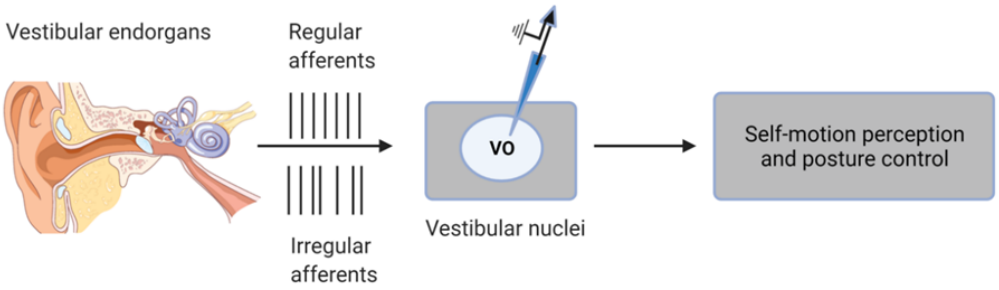

B.

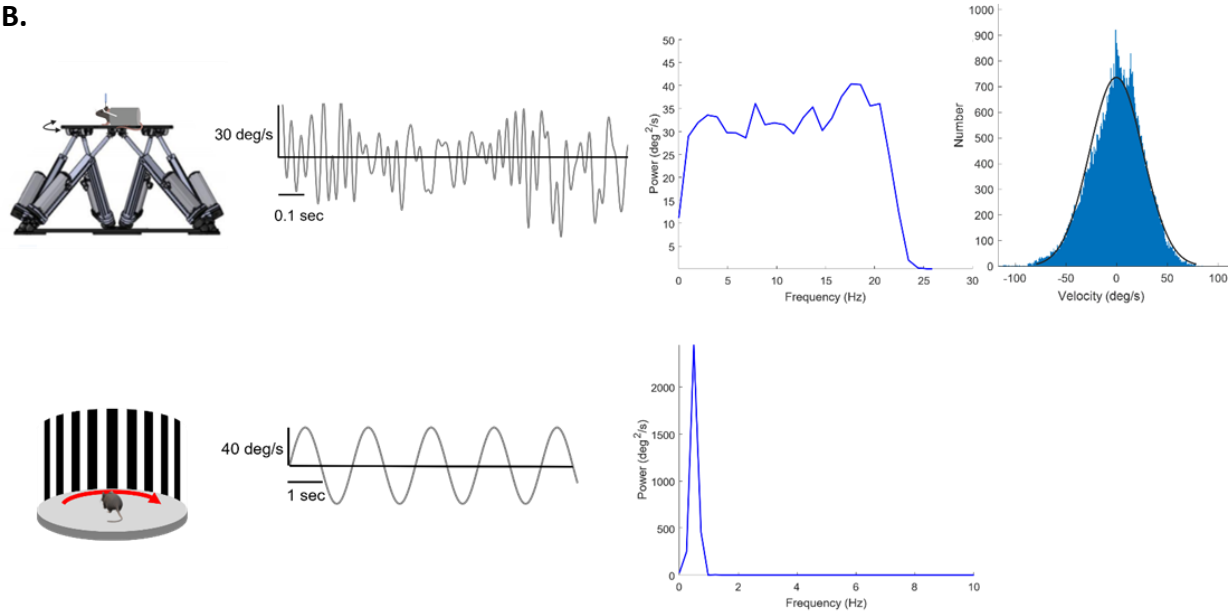

Fig. 2.2: Experimental setup and stimuli used. A. The general schematic of the vestibular pathway. Electrophysiological recordings were made from vestibular-only cells in the vestibular nuclei. B. Broadband (0-20 Hz) and sinusoidal stimuli (0.5 Hz) played on the hexapod and turntable, respectively, along with their time and frequency domain plots. The broadband noise had a gaussian distribution with a mean of -0.53 deg/s and a standard deviation of 27 deg/s.

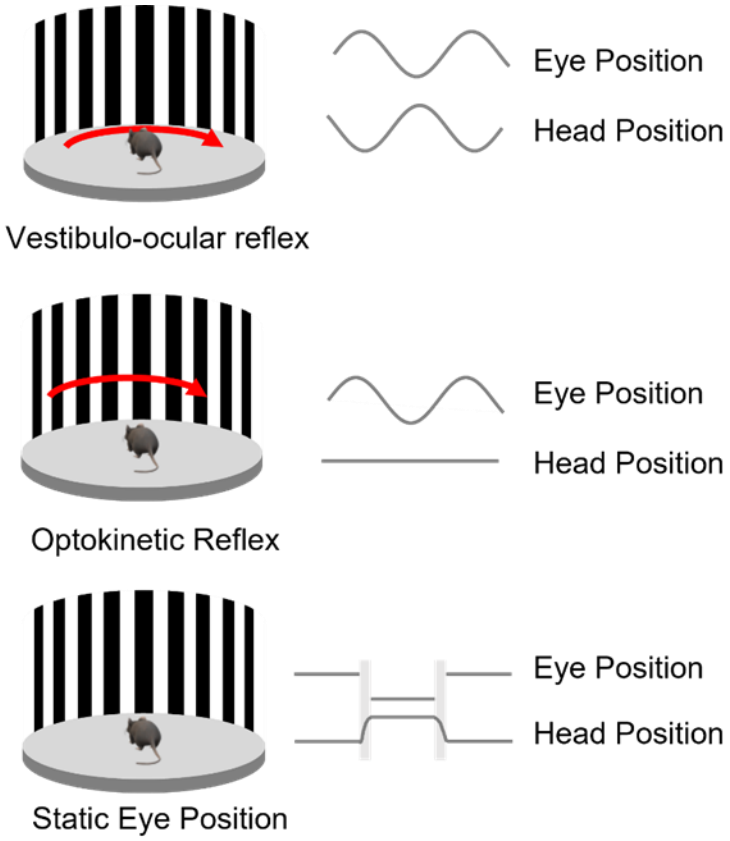

Fig. 2.3: Behavioral paradigms for dissociating eye and head movement sensitivity in the vestibular nuclei cells. During the vestibulo-ocular reflex paradigm, only the turntable was rotated in the yaw plane causing a change in head and eye position. In the optokinetic reflex paradigm, only the visual surround was moved and thus the head of the mouse was stationary, and the eye position changed. Lastly, for the static eye position paradigm, the eye was moved to different eccentric position by moving the turntable. In between the turntable movements, the eye and head positions were constant.

The movement of the turntable and visual surround in the first setup and the hexapod platform in the second setup was captured using gyrometers. The eye movements of the mice were recorded using the magnetic sensor implanted on the head of the mice. All the experiments were performed in the light. The neuropixel probe was lowered using the stereotaxic arm at a rate of 100 µm/min and secured in place by attaching it to the aluminum stereotaxic adapter

which was screwed to the probe holder (see Fig 2.1). The recordings were made at a depth of ~4.6 mm in the mouse brain.

2.2.3 Data acquisition

The 960-channel high-density neuropixel probes having 12 um x 12 um size titanium nitride electrodes with a uniform impedance of 149 ± 6 kΩ (mean ± SD) were used to record from the medial VN (MVN) (see Fig 2.4). VO neurons were identified by their robust responses to vestibular stimulation and showing no sensitivity to eye movements (Roy and Cullen, 2004). Data was acquired using the SpikeGLX acquisition system at 30kHz and band-pass filtered at 300-3000 Hz. The analog signals comprising of the head velocity and eye position were captured at 1000 Hz and low-pass filtered at 250 Hz.

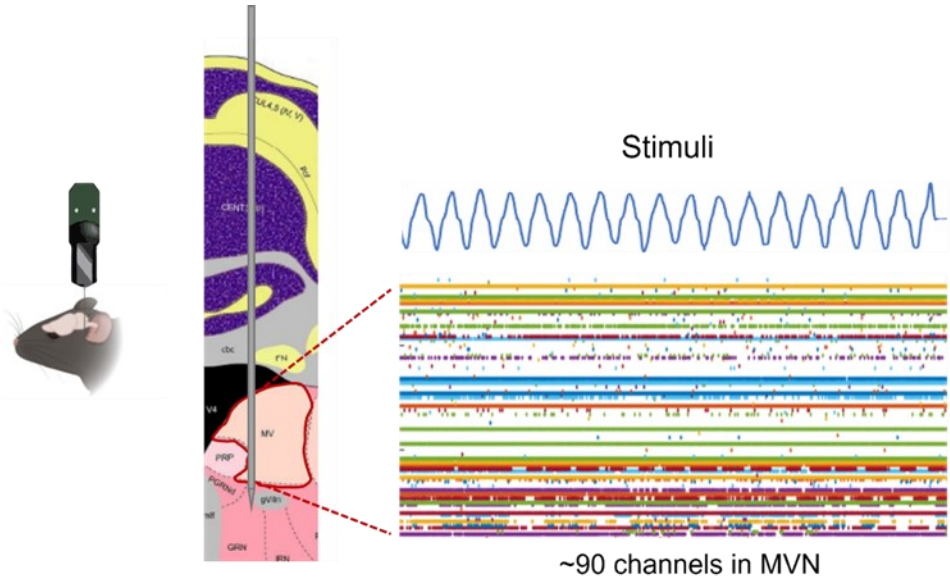

Fig. 2.4: Illustration of the ability of the neuropixel probe to record the simultaneous activity of many neurons in the medial vestibular nuclei (MVN) responding to sinusoidal stimuli. A total of ~90 out of 960 channels were present in the MVN with each site having a vertical and horizontal spacing of 20 and 16 µm, respectively, from one another.

2.2.4 Marking lesions

After the completion of the recording session and data acquisition, the neuropixel probe was removed and replaced with the stainless-steel electrode. The electrode was advanced to the same stereotaxic coordinates as the recording electrode using the stereotaxic arm. Electrolytic lesions were performed using a lesion-producing device (Stoelting). After lesions were made, animals were perfused with 4% paraformaldehyde, and coronal sections were cut and Nissl-stained. The localization of the lesion at the MVN was assessed using the shape of the fourth ventricle and the presence of abducens (see Fig 2.5).

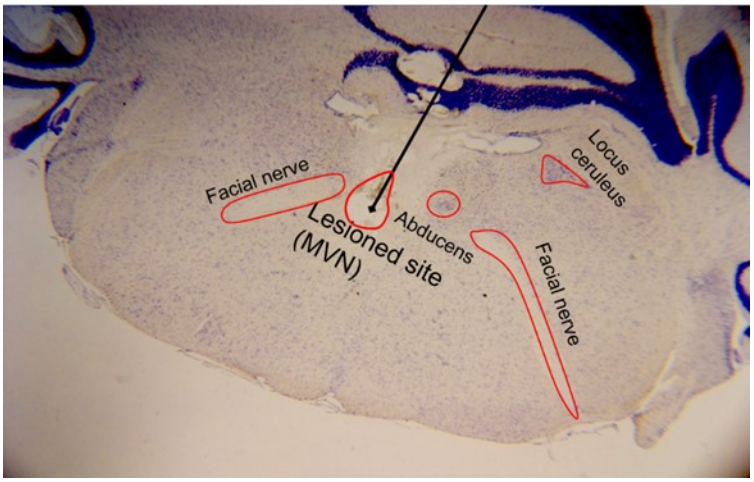

Fig. 2.5: Histological evaluation for confirming the location of the target recording site. The coronal section was approximately 6 mm caudal to the bregma where the lesioned site (medial vestibular nuclei) showed no Nissl staining.

2.2.5 Single unit data analysis

2.2.5.1 Spike sorting: Kilosort 2.0 was used for sorting the neuronal data. The phy GUI interface was used for visualizing the single unit data. Cells of interest were chosen by looking at their firing rate modulation to the VOR paradigm. The cross-correlogram of the single unit was checked to

make that there were no violations of the refractory period. Moreover, by looking at the amplitude versus the time plot, any drift in the data was detected. Specifically, neurons having a gaussian amplitude distribution were chosen. Interspike Intervals (ISIs) of the unit activities were also considered to avoid the inclusion of any multiunit activity in the data analysis.

Additionally, waveforms at the site of interest were verified to ensure the absence of any noise. For merging two units, the cross-correlogram plots, spike waveforms and ISIs were checked to ensure that it was the same unit. Moreover, to be sure of the presence of the same unit in a channel across different paradigms, the baseline firing rate was checked for consistency.

2.2.5.2 Baseline activity analysis of VO neurons: The binary spike train sequences obtained from Kilosort 2.0 for the units of interest were used for computing the ISIs and coefficient of variance (CV). CV, used to quantify the variability in the resting discharge, was computed as the ratio of the mean (μ) and standard deviation of the ISI. CV was normalized (CV*) to remove its dependence on the resting rate which was computed as (Goldberg et al., 1984):

$$CV^* = \left[\frac{CV}{0.7116\log(\mu) - 0.8248}\right]^{\frac{1}{0.00002\mu^3 - 0.0024\mu^2 + 0.0731\mu + 0.37}} \quad (1)$$

Here, μ was in seconds. The power spectrum of the VO neuron was computed using MATLAB's pwelch function with a sampling frequency of 1KHz.

2.2.5.3 VO cell tuning: The spike train obtained after sorting was convolved with a Kaiser window having a cut-off frequency equivalent to one greater than twice the frequency of the stimulus to compute the firing rate of the neuron (Sadeghi et al., 2007b). The firing rate of the cells was estimated from the stimulus, $s(t)$, using a least-squares linear regression model given by

$$fr_{estimated} = b + g.s(t - t_d), \quad (2)$$

where b was the baseline firing rate, g was the gain, and t_d was the latency (Sadeghi et al., 2007b). At least ten segments of the data were chosen for the computation and the parameters mentioned above were selected based on the best fit and having the maximum variance accounted for (VAF) (Sadeghi et al., 2007b). The VAF was calculated as:

$$VAF = 1 - \frac{[fr_{estimated}(t) - fr_{measured}(t)]}{var[fr_{measured}(t)]}. \quad (3)$$

Here, var was the variance and $fr_{measured}(t)$ was the actual firing rate (Roy and Cullen, 2001; Sylvestre and Cullen, 1999).

2.2.5.4 Estimation of MI and CF: To determine the amount of information which could be inferred about the stimuli from the neural response, MI was computed from coherence as follows (Massot et al.,2012):

$$C(f) = \frac{|P_{sr}(f)|^2}{P_{ss}(f)P_{rr}(f)} \quad (4)$$

$$MI = -log_2\big(1 - C(f)\big). \quad (5)$$

Here, $P_{sr}(f)$, $P_{ss}(f)$, and $P_{rr}(f)$ represented the cross-power spectrum of the stimuli and response, power spectra of the stimuli, and response, respectively, and $C(f)$ was the coherence. MI was calculated in bits per second per Hertz which was normalized by dividing it with the mean firing rate to compute the MI density.

To further quantify the fraction of the stimuli that could be successfully reconstructed from the neuronal spike train, the coding fraction (CF) was computed as follows (Gabbiani 1996; Rieke, 1996):

$$CF = 1 + \frac{\varepsilon}{\sigma_{stim}}, \tag{6}$$

where ε was the root mean squared error between the actual ($s(t)$) and estimated ($s_{reconst}(t)$) stimulus waveform and σ_{stim} was the standard deviation of the stimulus. The $s_{reconst}(t)$ was computed by convolving the spike train of the neuron with an optimal filter kernel $k(\tau)$ which minimized ε and was given by (Rieke, 1996):

$$s_{est}(t) = \int d\tau K(\tau)(t - \tau), \tag{7}$$

where $k(\tau)$ was the inverse Fourier transform of (Rieke, 1996; Dayan and Abbott, 2001):

$$K(f) = \frac{P_{sr}(-f)}{P_{rr}(f)}. \tag{8}$$

2.2.5.5 Computation of noise correlations between VO neuron pairs

In the study, 15 pairs of neurons were recorded simultaneously across five trials of sinusoidal 0.5 Hz stimuli. Each sine wave cycle was divided into 20 equal time bins, and the mean

firing rate was computed for each bin. The Pearson correlation coefficient (between 0 and 1) of the mean firing rate between the pair of neurons represented the signal correlation (Liu et al., 2013). In order to remove any correlations in the responses of the neuron pair due to the sinusoidal stimuli, their mean firing rates within each bin were z-score transformed across the five cycles. The Pearson correlation coefficient value between the z-scored mean firing rates generated the noise correlation between the neuron pairs (Liu et al., 2013).

To further evaluate how the resting variability of the neuron pair affected their noise correlation, the correlated CV was computed as (Metzen et al., 2015),

$$\overline{CV} = \sqrt{CV_{n1} \times CV_{n2}}, \quad (9)$$

where $CV_{n1}$and CV_{n2} were the CVs of the two neurons in the pair.

2.3 Results

This study aimed to understand the neural encoding of head movement by the VO neurons in mouse VN which are critical for maintaining balance, self-motion, and spatial orientation perception. To do so, single unit recordings were performed using the high-density neuropixel probes in the MVN of the mouse brain while it was subjected to passively-applied sinusoidal and broadband noise stimuli (see Methods and Fig 2.2). The dataset comprised of 18 VO neurons, and the isolation of the single units was successfully maintained across the highly dynamic stimuli conditions. The firing properties of the VO neurons including the gain, phase and variability in the resting discharge were analyzed and compared to regular and irregular

vestibular afferents in mice. Furthermore, the coherence, CF and MI were computed to estimate the amount of information conveyed by them at the behaviourally relevant frequency range of 0-20 Hz. Comparisons were also drawn with the monkey VO neurons. Additionally, to investigate population coding, noise correlation between the pairs of VO neurons was computed. Thus, applying information-theoretic measures to quantify the information transmitted by the VO neurons and analyzing their inter-neuronal variability as an ensemble helped shed light on the sensory processing and the neuronal connectivity in the mouse VN.

2.3.1 Spontaneous activity of VO neurons

In the present study, the resting activity of 10 VO neurons was analyzed, which averaged at 50.71 ±19.03 spikes/s (mean ± SD). For the characterization of the variability in the neuronal responses, CV and CV * were computed from the ISIs of the neuron spike trains. The CV of the mouse VO neurons (0.75±0.42) showed an inverse relationship with the baseline firing rate (see Fig 2.6A). Thus, to remove any dependence of the neural variability on the resting discharge, the normalized CV, also known as CV*, was computed using Eq. 1 (see Methods) and was found to be 0.52±0.18 as shown in Fig 2.6B. The ISI histogram and power spectrum of a typical VO neuron is illustrated in Fig 2.6C and D, respectively, which had a CV* of 0.39 and showed temporally whitened responses where the spike train was independent of the frequency.

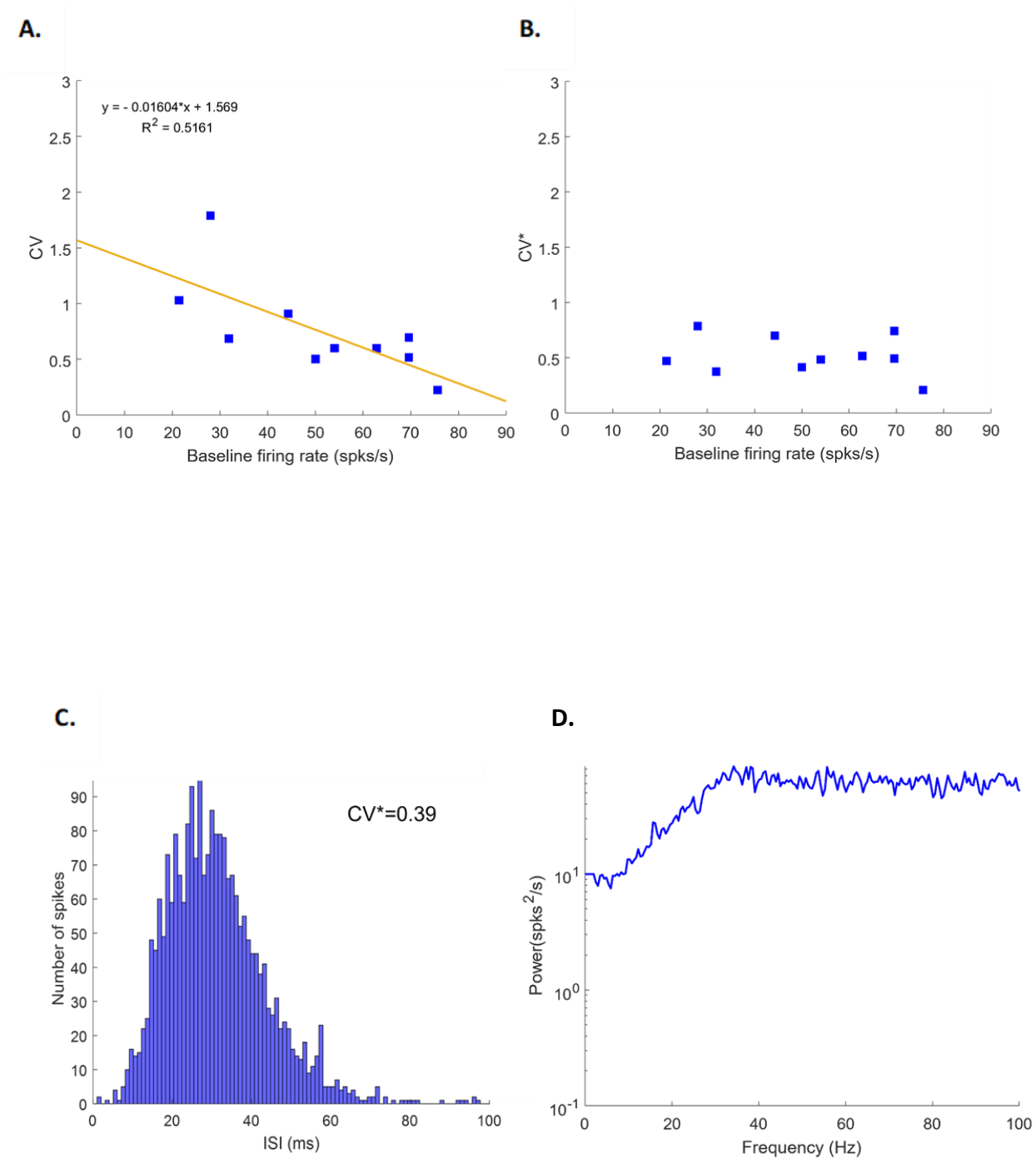

Fig. 2.6: Static firing properties of the mouse vestibular-only (VO) neurons (n=10). A. Relationship between CV and baseline firing rate showing a negative correlation. B. CV* as a function of the baseline firing rate showing an independent relationship. C. ISI histogram of an example VO neuron having a CV* of 0.39. D. Power spectrum of the same neuron showing less structure and Poisson firing statistics.

Overall, the static firing properties of mouse VO neurons showed considerable similarity with the monkeys. Massot et al. (2011) has previously reported the resting discharge of monkey VO neurons to be 56.2±24.6, which was not significantly different from the mouse VO neurons examined in this study [*P*=0.51, t-test, degrees of freedom (df) = 29; see Fig 2.7A]. Moreover, the responses of mouse VO neurons were more variable than the regular and irregular afferents innervating them from the periphery (see Fig 2.7B *inset*). It has already been shown by Lasker et al. (2008) that the average CV* for the mouse regular and irregular afferents was 0.05±0.02 and 0.35±0.13, respectively. However, the CV* of the mouse VO neurons was slightly lower but not significantly different from the monkey VO neurons (CV*=0.53±0.23) studied previously by Massot et al. (2011) (*P*=0.89, t-test, df=29; see Fig 2.7B). Additionally, like primates, the power spectrum of the mouse VO neurons indicated that the firing properties of the neurons closely followed a Poisson statistic (Holden, 1976, Cox and Lewis, 1966; Massot et al., 2011). Therefore, the results showed similar resting discharge properties of mouse and monkey VO neurons.

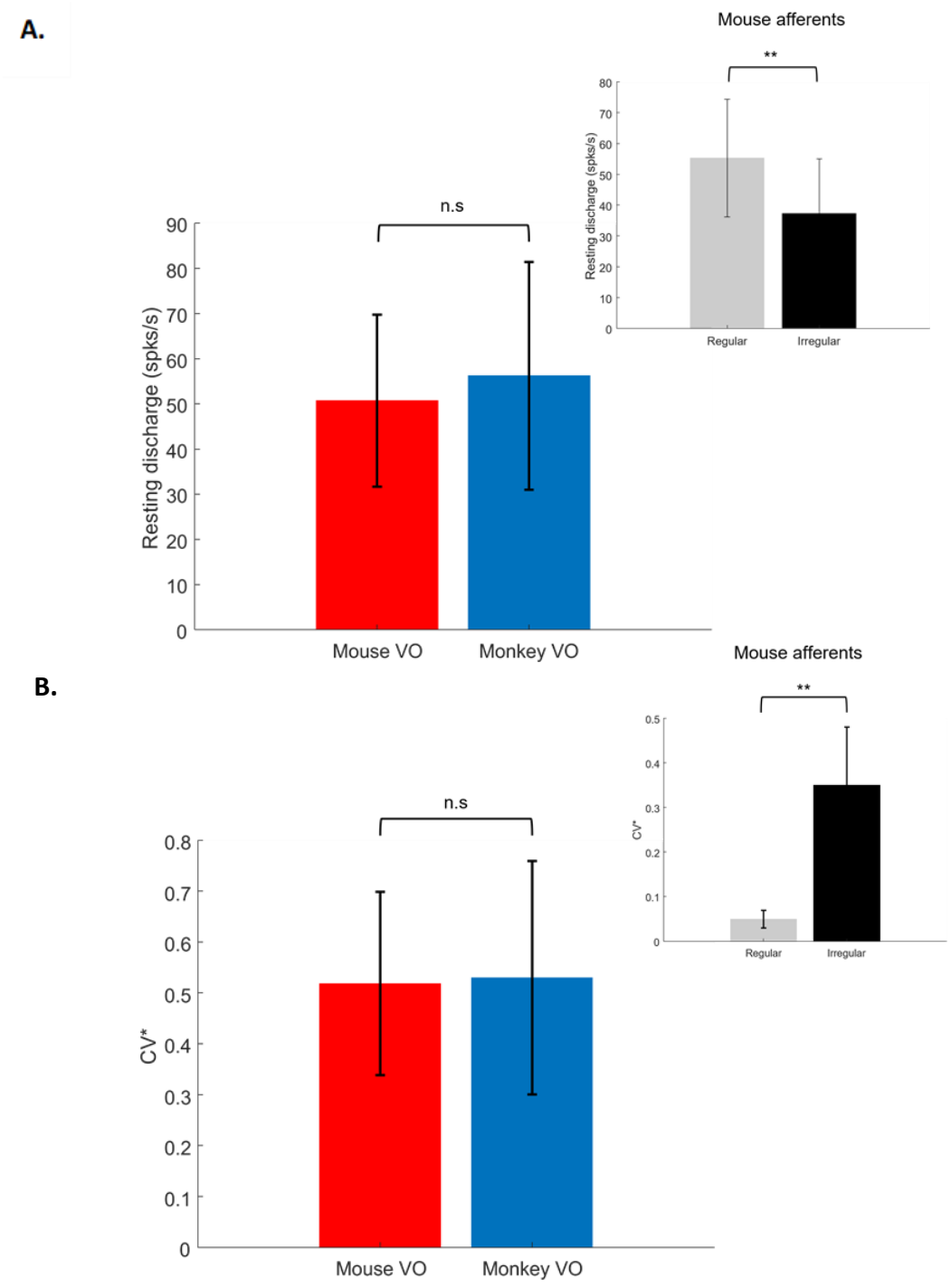

Fig. 2.7: Comparison of the resting discharge and CV* of mouse vestibular-only (VO) neurons with their afferents and monkey VO neurons. A. Bar plots with 1 SD error bars showing a comparison of the resting charge between the mouse and monkey VO neurons. B. Bar plots with 1 SD error bars showing a comparison of the CV* between the mouse and monkey VO neurons. Insets in the bar plots show a

comparison between mouse regular and irregular afferents. ** and n.s indicate statistical significance at P=0.01 and no significance, respectively, using a t-test.

2.3.2 VO cell responses to sinusoidal head movements

The dynamic responses of the VO neurons (n=10) were analyzed for 0.5, 1, and 2 Hz sinusoidal stimuli used previously by Beraneck and Cullen (2007). The cell population comprised of 4 type II and 6 type I neurons that increased their firing rate when the head was moved contralateral and ipsilateral to the recording site, respectively. By using a linear regression model, the gain and the phase of the VO neurons responding to sinusoidal rotations at 40 deg/s was computed, and the goodness of the fit was checked by calculating the VAF (see Eq. 2 and 3 in Methods). An example type I VO neuron showing head movement sensitivity during a 0.5 Hz VOR paradigm (head velocity sensitivity=0.37 spikes/s)/(deg/s), VAF=0.86), and no sensitivity to eye position during the SEP paradigm is shown in Fig 2.8.

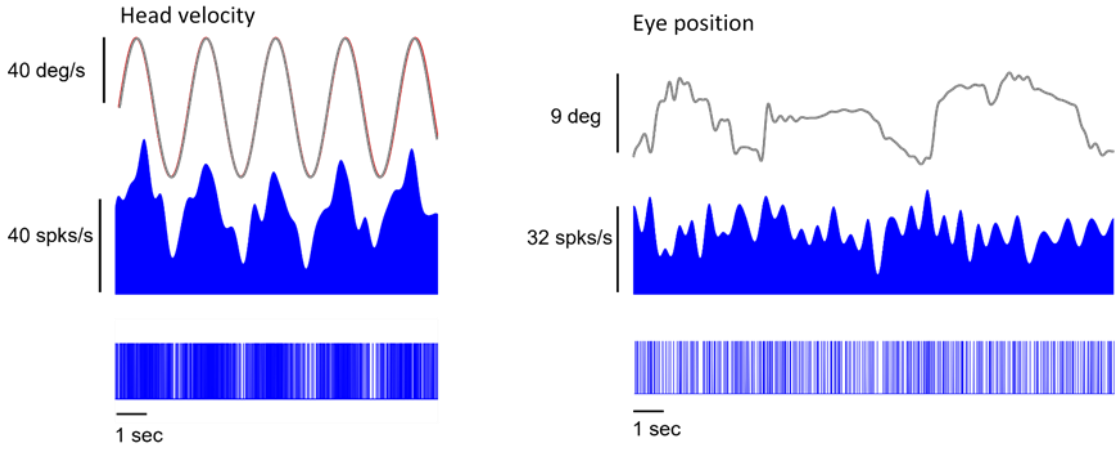

Fig. 2.8: Firing characteristics of mouse vestibular-only (VO) cells during sinusoidal head movements. An example VO cell responding to head movements [head movement sensitivity = 0.37 (spikes/s)/(deg/s); VAF = 0.86] but showing no change in its firing rate when the eye is moved to different eccentric positions during the static eye position paradigm.

While the gain values for the mouse VO neurons in the study were comparable to those reported by Beraneck and Cullen (2007), they were considerably higher than their regular and irregular afferents. Moreover, their overall sensitivity was lower than monkey VO neurons (*P*=0.019, t-statistic, df=29 at 2 Hz; see Fig 2.9A). Also, the mouse VO neurons showed higher phase leads with increasing frequencies than the afferents that were not significantly different from the monkey VO neurons (see Fig 2.9B). Thus, apart from gain, the dynamic response properties of the mouse and monkey VO neurons were common for frequencies up to 2 Hz.

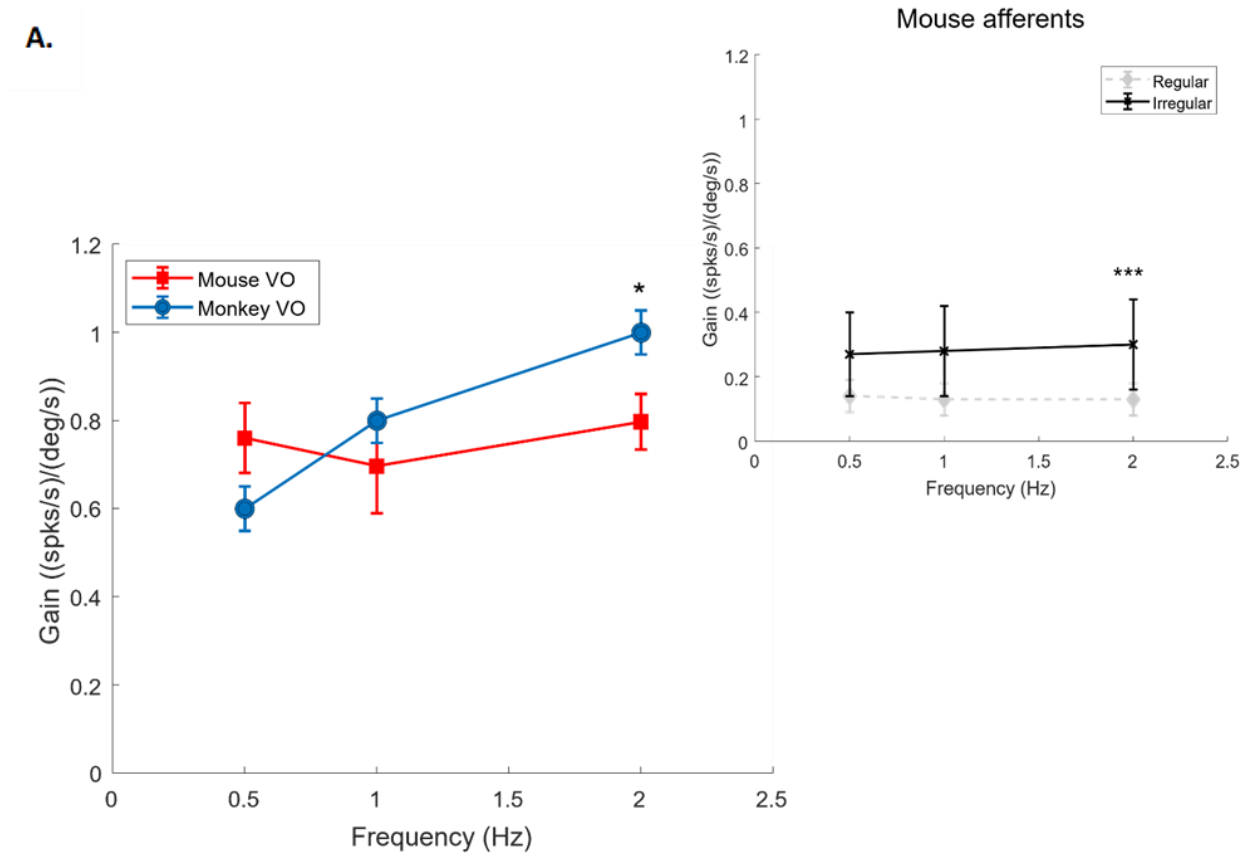

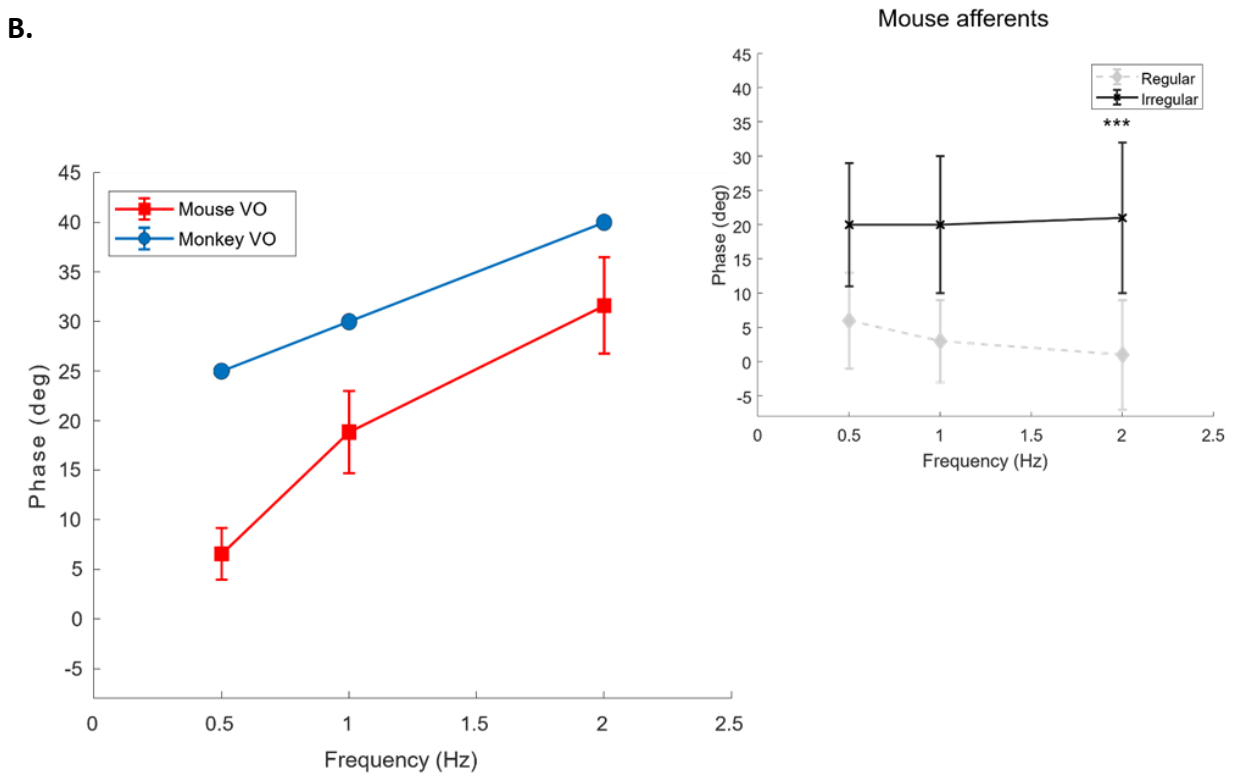

Fig. 2.9: Bode plot comparisons between mouse afferents, mouse vestibular-only (VO) (n=10), and monkey VO neurons. A & B. Gain vs frequency plots of mouse and monkey VO neurons. Mouse VO neurons showed higher gains than their afferents but overall lower gains than monkey VO neurons with increasing frequency. C and D Phase vs frequency plots of mouse and monkey VO neurons, respectively. Mouse VO neurons showed higher phase values than their afferents but overall lower phases than monkey VO neurons with increasing frequency. Insets show a comparison between mouse regular and irregular afferents. *** and * indicate statistical significance at P<0.005, and P<0.05, respectively, using a t-test.

2.3.3 Information transmission by mice VO neurons

To better understand the stimuli encoding in the VO neurons over the behaviourally relevant frequency range of 0-20 Hz (Carriot et al., 2017), the mouse was subjected to passively-applied broadband noise stimuli of 0 to 20 Hz with a mean of -0.53 deg/s and standard deviation of 27 deg/s using a highly dynamic hexapod (see Fig 2.2B). The VO neurons (n=3) showed a gain

of 1.1±0.45 (spks/s)/(deg/s). For computing the information transmitted by the VO neurons, the stimulus reconstruction technique used previously by Sadeghi et al. (2007) and Massot et al. (2011) was used where the spike train of the neuron was convolved with an optimal filter to reconstruct the head velocity signal (see Eq. 7,8 in Methods and Fig 2.10 *inset*). The fraction of the successfully reconstructed stimuli from the spike train across all the frequency components was quantified using the CF calculated using Eq. 6 (see Methods; 0.28 ±0.02, mean±1SE). An example mouse VO neuron showing poor stimulus reconstruction (CF=0.26) is shown in Fig. 2.10.

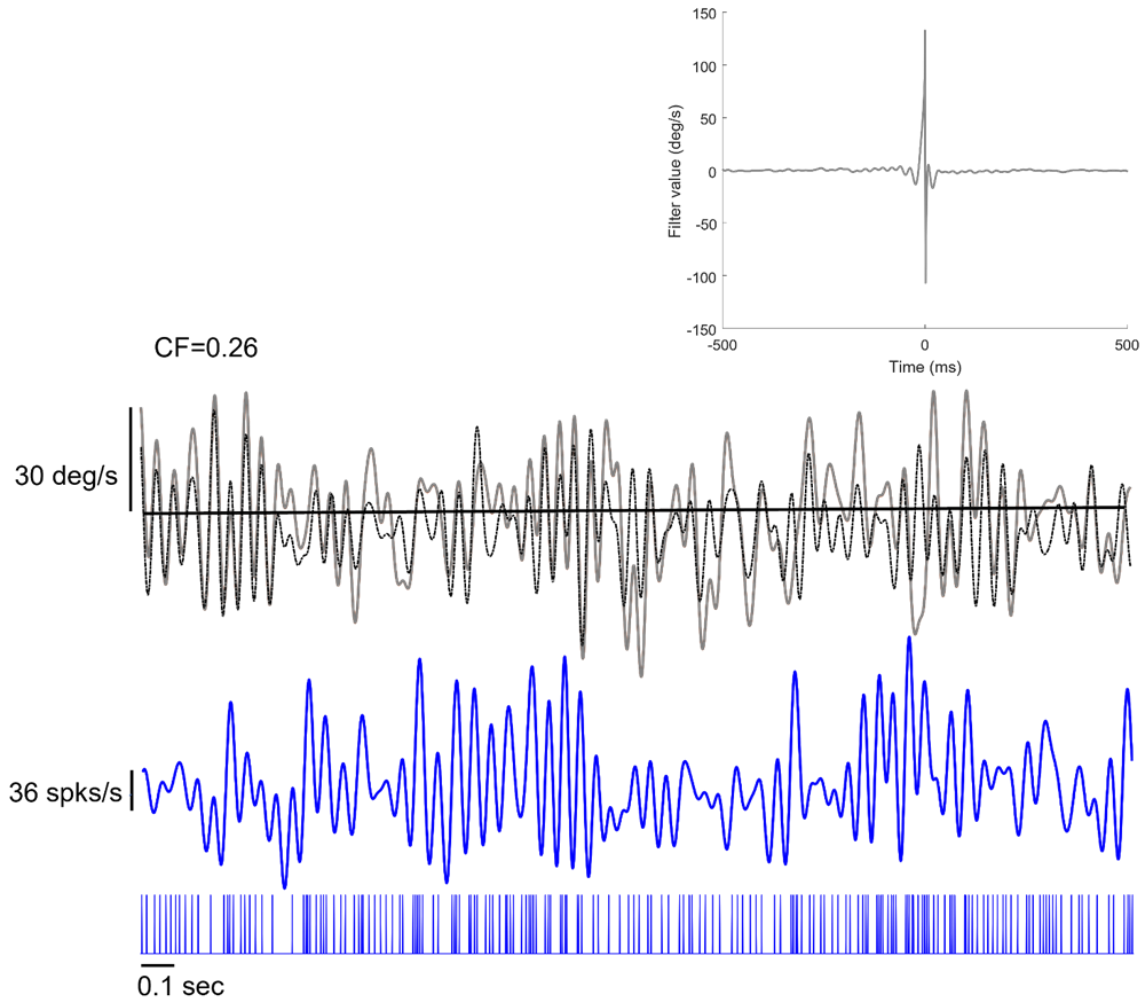

Fig. 2.10: Reconstruction of the stimuli for an example mouse vestibular-only neuron. The time-dependent reconstructed stimuli (black dotted line) and the original broadband stimuli (grey trace) gave a coding fraction (CF) of 0.26. The firing rate (blue trace) and the binary spike train are also shown. The inset shows the optimal filter waveform with which the spike train was convolved to compute the reconstructed stimuli.

Furthermore, to compute the information conveyed by the mouse VO neurons at the individual frequency components, the MI density between the neuronal spike train and the broadband head velocity stimulus was computed using Eq. 5 (see Methods) as a function of the temporal frequency and was approximately 0.016 bits/spks/Hz at 20 Hz as shown in Fig 2.11A.

It has been previously reported by Massot et al (2011) that the MI density showed a similar increasing trend from 0 to 20 Hz in monkey VO neurons. In accordance with the results obtained by Sadeghi et al. (2007) and Massot et al. (2011), the CFs of the mouse VO neurons were lower than the monkey regular and irregular afferents (see Fig 2.11B *inset*). However, the mouse VO neurons showed slightly higher but not significantly different CFs than monkey VO neurons, as shown in Fig 2.11B (P=0.076, t-test, df=22). Hence, the results highlighted a similar information transmission capacity in the VN of both the species for frequencies ranging from 0 to 20 Hz.

Despite having lower gains and similar fluctuations in their baseline activity compared to monkey VO neurons, the similar MI densities and CFs of the mouse VO neurons can be hypothesized to be due to the presence of non-linearities in their responses. Thus, future studies focused on the computation of the coherence between the neural responses and the stimulus and neural response to repeated presentations of the same stimulus would be consequential (Roddey et al., 2000; Jamali et al., 2019). The hypothesis could be further bolstered if the neurons

show temporal coding on a millisecond timescale computed using the Victor-Purpura and van Rossum spike distance metrics (see section 1.5.2 of chapter 1) used previously by Jamali et al. (2016).

A.

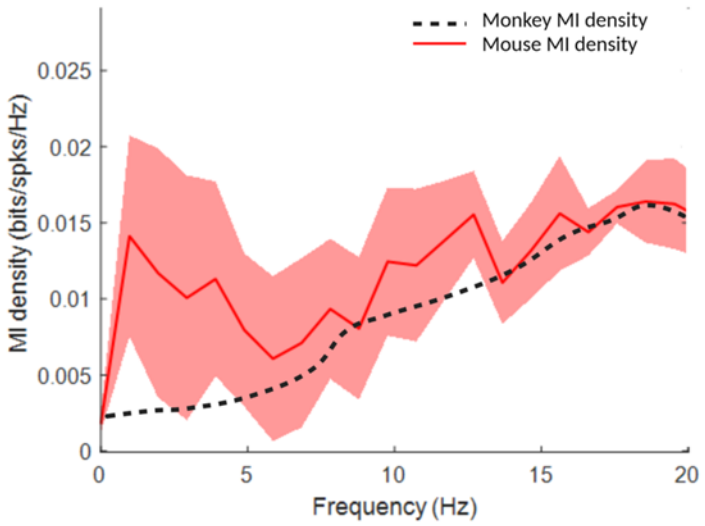

B.

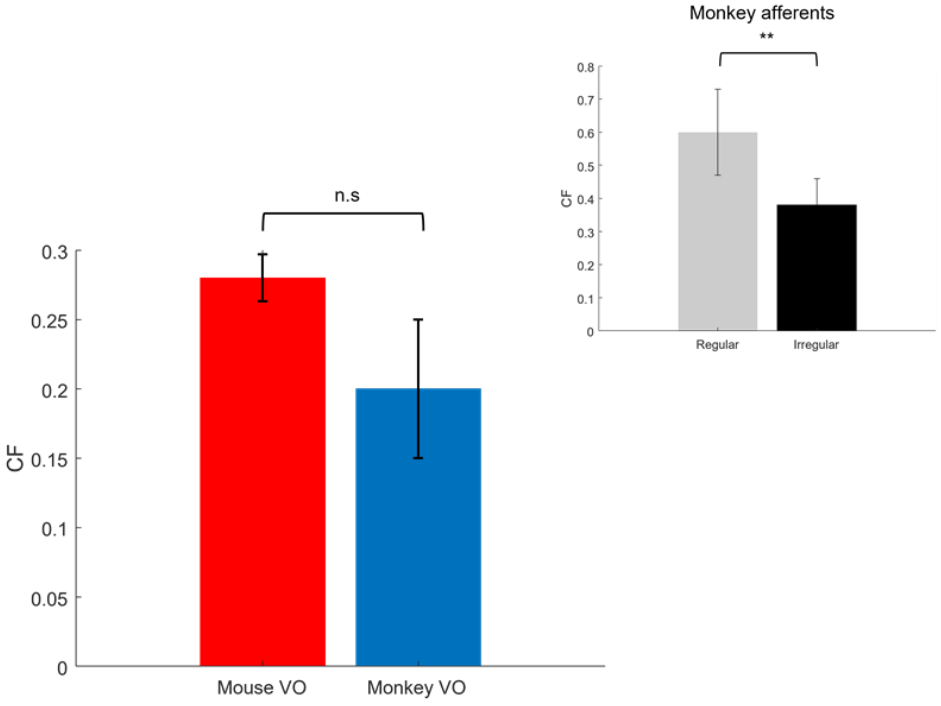

Fig. 2.11: Mutual information (MI) density and comparison of the coding fractions (CFs) between mouse (n=3) and monkey vestibular-only (VO) neurons. A. Variation in the population-averaged MI density for mouse and monkey VO neurons across 0-20 Hz frequency range. MI density for mouse and monkey VO neurons was comparable. B. Comparison of CF between monkey and mouse VO neurons. The difference between the CFs of mouse and monkey VO neurons was not significant. Inset shows the CFs obtained for the monkey regular and irregular afferents. ** and n.s indicate statistical significance at P<0.01, and no significance, respectively, using a t-test.

2.3.4 Noise correlations between mouse VO neuron pairs

The high-density neuropixel probes provide a unique advantage of high spatial resolution and the simultaneous capture of many single units, thereby making the study of population coding readily amenable. Thus, in this research investigation, a total of 15 pairs of mouse VO neurons were analyzed for five trials during a 40 deg/s sinusoidal stimulation at 0.5 Hz. The tuning similarity for the neural population, also known as the signal correlation, was estimated by computing the Pearson correlation of their mean firing rate across the trials and was found to be 0.95±0.022 (mean±1 SD). To compute the noise correlations, the mean firing rates were z-score transformed across the trial cycles to remove any variability in the neural responses due to the stimuli and was estimated to be 0.21±0.23. Two example pairs of simultaneously recorded neurons separated by a distance of 0.42 mm and 0.04 mm and showing a signal correlation of -0.93 and 0.94 (P < 1e-5) and a noise correlation of 0.12 (P=0.22) and 0.33 (P=0.001), respectively, are shown in Fig 2.12. Moreover, to examine the relationship between the noise correlation and the co-variability between the neuron pairs, the correlated CV was computed using Eq. 9 (see Methods), which showed a insignificant negative correlation of -0.21 (P=0.45, see Fig 2.13).

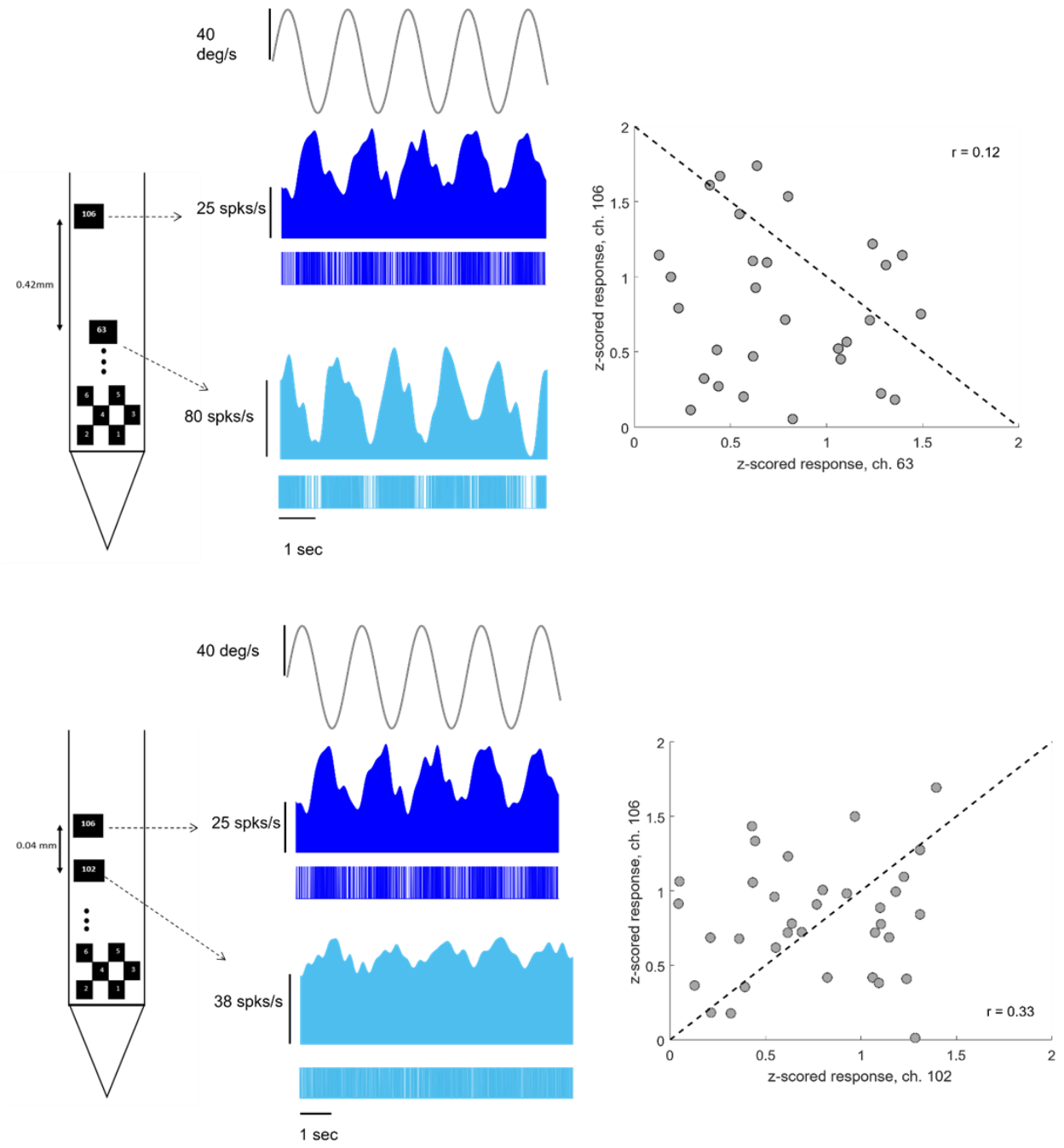

Fig. 2.12: Noise correlation between mouse vestibular-only (VO) neurons. The values for excess synchrony for the far (0.42 mm) and near (0.04 mm) example pair of VO neurons showing a noise correlation r of 0.12 (P=0.21) and 0.33 (P=0.001), respectively, during a sinusoidal stimulation of 0.5 Hz.

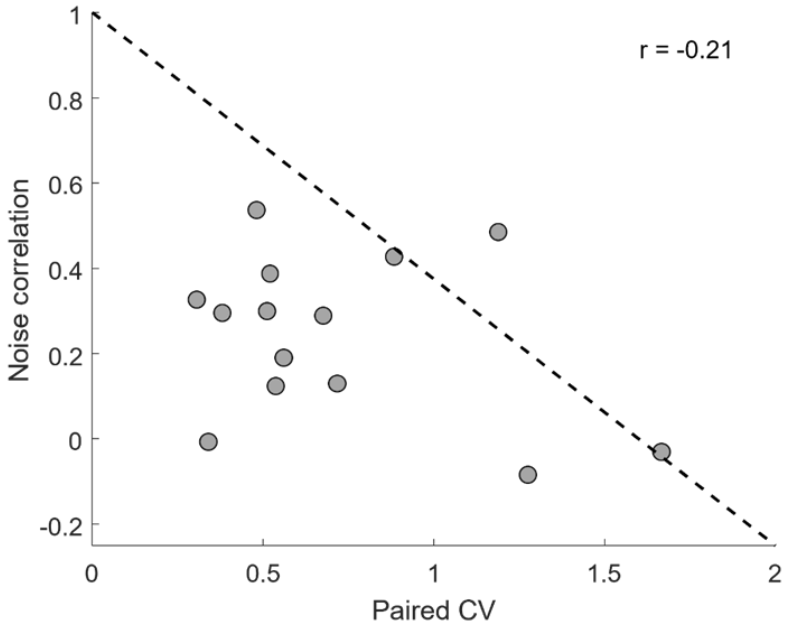

Fig. 2.13: Relationship between correlated variability (CV) and noise correlation between the pairs of vestibular-only neurons recorded simultaneously using neuropixel probes at 0.5 Hz sinusoidal stimulation (n=15 pairs). The negative correlation (r=-0.21) was not found to be significant (P=0.45).

In monkeys, weak correlations between the inter-neuronal variability of the VN neurons have been reported previously by Liu et al., 2013 using low-density probes. While the noise correlation values between the individual pairs of neurons in this study were comparable to those reported by Liu et al. (2013), the population-averaged correlation values were significantly greater than zero since the size of the neuron population was smaller. More specifically, Liu et al. (2013) studied a total of 47 pairs of VN neurons where the positive and negative noise correlations between the neuron pairs canceled one another, thus making the population averaged value insignificant from zero. Moreover, in this study, neuron pairs no more than 1.9 mm apart were studied, unlike Liu et al. (2013), where the distance between the pairs was as

large as 4 mm. Thus, the similarity in noise correlations between pairs of individual neurons in mice and monkeys underscored the presence of a common neural circuitry in the two species.

2.4 Discussion

2.4.1 Summary of the results

In this scientific investigation, the firing statistics, including the gain, phase, and variability in the resting discharge of the mouse VO neurons was determined for the sinusoidal stimuli of 0.5, 1, and 2 Hz, and broadband noise stimuli containing frequencies from 0 to 20 Hz. The results of the study highlighted the similarity in the variability of the baseline response activity and lower gains of the mouse VO neurons as compared to NHP VO neurons. Moreover, no significant differences were found in the MI densities and the percentage of stimuli waveform, which could be reconstructed from their spike trains (CF) for the broadband noise stimuli. Additionally, to investigate population coding, pairwise noise correlation was computed between the mouse VO neurons and was found to be low as previously shown in monkeys.

2.4.2 Comparable MI and CFs between mouse and monkey VO neurons

Sadeghi et al. (2007b) and Massot et al. (2011) have shown that the irregular afferents and VO neurons in primates show higher baseline variability than regular afferents. Specifically, the VO neurons showed the highest variability in their neural responses, thereby showing poor CFs and signal-to-noise ratios. However, as inferred from the MI density plots, the amount of information encoded by them increased at higher frequencies, indicating their ability to encode

highly transient movements successfully. Moreover, Mitchell et al. (2018) showed that this resting discharge variability contributed to the whitening responses of the VO neurons, leading to optimized coding as the information carried by their spike trains about the stimuli reached near its maximum value. While it was previously assumed that the irregular afferents and VO neurons used rate codes (Sadeghi et al., 2007b; Massot et al., 2011), in the breakthrough study by Jamali et al. (2016) on primates, it was established that the response variability of these neurons enabled them use precise spike timing on the order of milliseconds (~6 milliseconds) to encode the detailed time course of the high frequency stimuli.

In the mouse, there are two reasons to believe that their VN neurons would encode less information since they have: 1) lower gains and 2) similar resting discharge variabilities, as compared to NHPs (Beraneck and Cullen, 2007). Indeed, Lasker et al. (2008) observed low sensitivities in the mouse vestibular afferents synapsing directly in the VN. Furthermore, as explained by Beraneck and Cullen (2007), the low eye and head movement gains of the mouse VN neurons could be ascribed to the low-inertia of their oculomotor plant, to increase their linear range of encoding head movements, or to the low requirement of gaze control because they are afoveates.

Nonetheless, according to the results of this study, during broadband noise stimulation, the mouse VO neurons showed comparable MI densities and CFs to primates. I hypothesize that the mouse VO neurons show low trial-to trial variability in their responses which could be confirmed by computing the non-linearity in their responses and precision in their spike timing

in the future studies. Furthermore, a similar study analyzing the activity of a larger population of not only mouse VO, but also eye-sensitive cells during passively-applied naturalistic head movement stimuli would provide a better understanding of their sensory processing.

2.4.3 Anatomical influence of the VN on low noise correlation between VO neurons

Studies have shown that the vestibular afferents have collateral branches that contact many VN cells (Ishizuka et al., 1982; Sato et al., 1989; Newlands and Perachio, 2003). Besides receiving a common input, Condorelli et al. (2000) and Beraneck et al. (2009) have shown the presence of connexing-36 gap junctions between the VN neurons, which could lead to electrical coupling. However, as per the results of this study I found poor anatomical and electrical coupling between the VO neurons, which is consistent with the observation made by Liu et al. (2013) in the monkey VN. The results of this study also support the idea that a single VO neuron is innervated by many afferents, thereby receiving diverse inputs (e.g., Carriot et al., 2015; Yakushin et al., 2006; reviewed in Uchino et al., 2005).

It was interesting to note local synchrony between the pairs of neurons in the nucleus prepositus, a region very close to the VN (Dale and Cullen, 2015). Nucleus prepositus neurons showed an average synchrony of 3.6±1.0 and 4.4±0.8% for contralateral to central and central to ipsilateral fixations, respectively. Also known as the oculomotor integrator, the nucleus prepositus contains many recurrent projections for computing the eye position signal from the eye velocity input, thus explaining the excess synchrony between its neurons. Such an integration also occurs in the VN which comprises of the velocity storage network for maintaining the

reflexive performance and perception of self-motion during slow and sustained head motion (reviewed in Angelaki and Cullen, 2008). However, the integration of the semi-circular canal afferent input is mediated by long-range reciprocal connections between the VN and the cerebellum, due to which lack of noise correlation exists between its neurons.

Thus, I predict that the anatomy of the VN prevents any correlation between its neurons. This speculation can be further confirmed by using a larger neural population stimulated at frequencies up to 20 Hz, where the noise correlations should still be negligible even though the neural sensitivity to the stimuli would increase at higher frequencies.

2.5 Conclusion

Altogether, the results of my study highlight for the first time the similarity in the neural variability and the encoding of the behaviourally pertinent frequencies between the mouse and monkey VO neurons. By using information theory metrics like MI density and CFs, in this research investigation I successfully computed the information transmitted by the mouse VO neurons during broadband noise stimulation. Moreover, I examined the population coding and inter-neuronal fluctuations in the activity of the mouse VO neurons by taking advantage of the multiple high-quality single units recorded simultaneously on the neuropixel probe. Thus, this study on mice, one of the leading animal models in biomedical research, marked the first step in quantifying the first stage of their central vestibular processing, understanding the downstream decoding of the stimuli, and inferring the neural circuitry of their VN.

Chapter 3

3.1 General discussion

The aims of this research study were two-fold: i) to understand and quantify the neural encoding of vestibular stimuli containing the behaviorally relevant frequency range of 0 to 20 Hz, and ii) to study population coding by determining the presence of any pairwise noise correlations in the mouse VO neurons.

The study's goals were achieved by first characterizing the static and the dynamic properties of the mouse VO cells. More specifically, as a part of the first goal, the resting discharge variability, the power spectrum of the neural responses, and the gain and phase during sinusoidal stimulation were assessed and compared with the mouse vestibular afferents and non-human primate (NHP) VO neurons. Moreover, I analyzed the responses of the mouse VO neurons during broadband noise perturbation and quantified the information conveyed by them by computing the mutual information shared between the spike train and the stimulus, and the fraction of the stimulus which could be successfully reconstructed from the spike train, also known as the coding fraction.

For the second goal, I examined the simultaneous activity of pairs of mouse VO neurons captured on the neuropixel probe to compute the noise correlations between them. The

implications of the results on the early and higher-order vestibular stimuli processing in the mouse are elucidated below.

3.1.1 Implications for the vestibular pathways mediating posture and self-motion perception

During everyday activities, we can successfully discriminate between voluntary and externally applied motion. This distinction between self and externally-generated movements has been shown to occur at the first stage of central vestibular processing, namely in the VO neurons of the vestibular nuclei (VN) (Roy and Cullen, 2004; Brooks and Cullen, 2014), which in turn send projections to the spinal cord and the cortex via the thalamus and is reciprocally interconnected with the cerebellum (see Fig 1.2).

VO neurons send signals to several spinal cord levels via the vestibulospinal and reticulospinal tracts (Goldberg et al., 2012). Both the tracts make significant contributions towards mediating vestibulospinal neck and limb reflexes by synapsing with the motorneurons and interneurons of the spinal cord to generate reflexive contractions in the musculature in the absence of self-generated movements to stabilize posture in response to unexpected head motion (Goldberg et al., 2012). In contrast, the efficacy of these vestibulospinal pathways is markedly reduced (>70%) during voluntary head movements (reviewed in Cullen, 2019). This reduction is logical since it gates out the generation of reflexive stabilizing movements that would oppose the intended movement relative to space.

Additionally, VO neurons in monkey also send direct projections to the ventroposterior thalamus (Marlinski and McCrea 2009). This posterior thalamic pathway has been shown to relay vestibular information to the cortical areas such as the parietoinsular vestibular cortex (Büttner and Lang, 1979; Grüsser et al., 1990; Magnin and Fuchs, 1977), leading to the perception of self-motion. Similar vestibular-sensitive cells have also been reported by Hennestad et al. (2021) in the retrospinal, primary somatosensory, motor, and posterior-parietal cortex of mice.

Finally, it is noteworthy that the VN is reversibly interconnected with the cerebellum, and that VO neurons receive projections from the rostral fastigial nucleus (rFN) of the cerebellum (Batton et al., 1977). Shadmehr et al. (2010) has proposed that motor learning occurring in the cerebellum not only fine-tunes the motor responses but is also driven by a sensory prediction error. This error, computed in the cerebellum, occurs when there is a mismatch between the incoming and the anticipatory sensory input and suppresses the activity of the VO neurons during self-generated movements (Cullen and Brooks, 2014). In the absence of a mismatch, the activity of the VO neurons is disinhibited and the vestibulospinal reflexes are facilitated.

As established by the results of my study, mouse VO neurons transmit comparable information, relative to their monkey counterparts, about highly dynamic head movement stimuli encountered during natural behaviors. I postulate that this such reliable transmission is consequential for self-motion perception and postural control in mice as in monkeys. However, it is noteworthy that the current study only used artificial stimuli to investigate the information transmitted by the mouse VO neurons. I propose that future work using naturalistic vestibular

stimuli experienced by mice during exploring, running, jumping, and grooming will provide further insights into the sensory processing occurring in the VN and its impact on the higher-order functions.

3.1.2 VN neurons contribute to the head direction network for spatial navigation

To be able to satisfactorily explore our surroundings, the knowledge of the current location and self-orientation is critical, requiring visual and nonvisual cues, including vestibular and proprioceptive input. It has been shown in monkeys that the VN also communicates with the cortex via a second anterior thalamocortical pathway in addition to the posterior thalamocortical pathway mentioned above (Hitier et al., 2014; Shinder and Taube, 2010). In the anterior thalamocortical pathway, the VN projects via a series of brainstem nuclei, namely, the nucleus prepositus, supragenual nucleus, and the dorsal tegmental nucleus, to the lateral mammillary nucleus projecting to the anterodorsal thalamic nucleus. The prevailing view is that vestibular input from the VN is essential for the computation of the head direction (HD) signal that is characteristic of neurons in the anterior thalamocortical pathway (reviewed in Taube and Cullen 2017). In turn, anterodorsal thalamic nucleus projections propagate this HD signal to the higher brain areas like the dorsal presubiculum, and the entorhinal cortex, where visual information is integrated to provide us with our sense of direction (reviewed in Taube and Cullen, 2017).

However, this prevailing view of signaling between the VN and the cortex can be challenged because the activity the VO neurons in the VN neurons is suppressed during active movements (Roy and Cullen, 2004; reviewed in Taube and Cullen, 2017). Consequently, as Taube

and Cullen (2017) postulated, the angular head velocity signal must be weighed up to compute directional heading successfully. Nevertheless, another class of VN neurons in the NHPs, namely the position-vestibular-pause (PVP) neurons, encode eye and head movement during active and passive movements for gaze stabilization (reviewed in Cullen and Roy, 2004). The PVP neurons send projections to the abducens nucleus and the prepositus, which responds primarily to eye movements and outputs position and velocity information of the eye in the head (McCrea et al., 1987; Taube and Cullen, 2017). Thus, an integration of the head and eye movement information in nucleus prepositus might explain the computation of the HD signal in monkeys (Taube and Cullen, 2017).

Nevertheless, to date, no study in mice has investigated the output of the nucleus prepositus. Moreover, the eye-sensitive (ES) cells in the mouse VN encode not only eye and head but also neck movements and might use egocentric information (i.e proprioceptive and motor efference copy) to develop an internal representation of the heading direction (Beraneck and Cullen, 2007; Medrea and Cullen, 2013). Thus, further investigation of the ES cells and their projections to the subcortical brain areas like the nucleus prepositus would help gain insights into the computation of the HD signal in the mouse model during active and passive movements.

3.1.3 Consequences of low noise correlations on vestibular stimuli decoding

Excess synchrony and noise correlations between neurons have been considered both beneficial and detrimental to the sensory encoding of stimuli based on the behavioral context and the region of the brain. On one hand, correlation in the inter-neuronal variability has been

seen in the retinal ganglion cells of mice where their excitatory and inhibitory inputs are balanced and cancel out one another, thereby preserving the original stimuli signal (Cafaro and Rieke, 2010). On the other hand, uncorrelated variability among neurons would cancel out during population summation and the stimuli signal could be consequently recovered, as seen previously during active whisking in mice by Poulet and Petersen (2008), and attention in monkey V4 neurons by Cohen and Maunsell (2009).

For a homogenous population of neurons, having independent noise which averages out to zero is crucial for the successful decoding of the stimuli by the downstream areas. Indeed Liu et al. (2013) has reported negligible population-averaged noise correlations among the VN neuron population in monkeys. Since mice share similar firing rate characteristics with primates, despite having lower gains, it can be predicted that they also show low noise correlations among their VN neuron pairs.

In the present study, the noise correlations between individual pairs of neurons were comparable to those reported by Liu et al. (2013) in the monkey VN, however, unlike the afore-mentioned study, the population average was not significantly different from zero. Thus, future work examining a larger population of simultaneously recorded VN neurons where a larger distance separates the pairs would provide a better understanding on how the neuronal fluctuations affect the downstream decoding of the stimuli in the mouse model.

3.2 Concluding remarks

Given that the VN, receiving primary input from the vestibular afferents and forming the first stage of central processing, sends projections to several brain regions, which bring about reflexive movements and perception of self-motion and spatial orientation, studying its information transmission is essential. However, information processing in the VN of the mouse, one of the most significant animal models in neuroscience, has not yet been quantified in the frequency range of natural head movements. Therefore, the goal of my study was to extend the approaches previously used to understand neural coding in early vestibular pathways in monkeys (Massot et al. 2011), by using information theory to quantify the information conveyed by the mouse VO neurons during broadband noise perturbation containing frequencies from 0 to 20 Hz. Moreover, an understanding of the downstream decoding of the vestibular stimuli was gained by evaluating noise correlations between the pairs of VO neurons. Taken together, the findings of my master's research thesis constitute an important first step in understanding the encoding and decoding of the vestibular stimuli, and the neural connectivity of the VN in mouse, one of the most extensively-studied animal model in neuroscientific research.

References

Abbott, L. F., & Dayan, P. (2005). *Theoretical neuroscience: Computational and mathematical modeling of neural systems.* MIT Press.

Aldworth, Z. N., Dimitrov, A. G., Cummins, G. I., Gedeon, T., & Miller, J. P. (2011). Temporal encoding in a nervous system. *PLoS Computational Biology, 7*(5), e1002041.

Angelaki, D. E., & Cullen, K. E. (2008). Vestibular system: The many facets of a multimodal sense. *Annual Review of Neuroscience, 31*(1), 125-150.

Attneave, F. (1954). Some informational aspects of visual perception. *Psychological Review, 61*(3), 183-193.

Averbeck, B. B., Latham, P. E., & Pouget, A. (2006). Neural correlations, population coding and computation. *Nature Reviews Neuroscience, 7*(5), 358-366.

Barlow, H. (2001). Redundancy reduction revisited. *Network: Computation in Neural Systems, 12*(3), 241-253.

Batton, R. R., Jayaraman, A., Ruggiero, D., & Carpenter, M. B. (1977). Fastigial efferent projections in the monkey: An autoradiographic study. *The Journal of Comparative Neurology*, *174*(2), 281-305.

Beraneck, M., & Cullen, K. E. (2007). Activity of vestibular nuclei neurons during vestibular and Optokinetic stimulation in the alert mouse. *Journal of Neurophysiology, 98*(3), 1549-1565.

Beraneck, M., Uno, A., Vassias, I., Idoux, E., De Waele, C., Vidal, P., & Vibert, N. (2009). Evidence against a role of gap junctions in vestibular compensation. *Neuroscience Letters, 450*(2), 97-101.

Britten, K. H., Newsome, W. T., Shadlen, M. N., Celebrini, S., & Movshon, J. A. (1996). A relationship between behavioral choice and the visual responses of neurons in macaque MT. *Visual Neuroscience, 13*(1), 87-100.

Brooks, J. X., & Cullen, K. E. (2014). Early vestibular processing does not discriminate active from passive self-motion if there is a discrepancy between predicted and actual proprioceptive feedback. *Journal of Neurophysiology*, *111*(12), 2465-2478.

Büttner, U., & Lang, W. (1979). The Vestibulocortical pathway: Neurophysiological and anatomical studies in the monkey. *Progress in Brain Research*, 581-588.

Cafaro, J., & Rieke, F. (2010). Noise correlations improve response fidelity and stimulus encoding. *Nature*, *468*(7326), 964-967.

Carriot, J., Jamali, M., Brooks, J. X., & Cullen, K. E. (2015). Integration of canal and otolith inputs by central vestibular neurons is Subadditive for both active and passive self-motion: Implication for perception. *Journal of Neuroscience, 35*(8), 3555-3565.

Carriot, J., Jamali, M., Chacron, M. J., & Cullen, K. E. (2014). Statistics of the vestibular input experienced during natural self-motion: Implications for neural processing. *Journal of Neuroscience*, *34*(24), 8347-8357.

Carriot, J., Jamali, M., Chacron, M. J., & Cullen, K. E. (2017). The statistics of the vestibular input experienced during natural self-motion differ between rodents and primates. *The Journal of Physiology, 595*(8), 2751-2766.

Cohen, M. R., & Maunsell, J. H. (2009). Attention improves performance primarily by reducing interneuronal correlations. *Nature Neuroscience*, *12*(12), 1594-1600.

Cohen, M. R., & Kohn, A. (2011). Measuring and interpreting neuronal correlations. *Nature Neuroscience, 14*(7), 811-819.

Condorelli, D. F., Belluardo, N., Trovato-Salinaro, A., & Mudò, G. (2000). Expression of Cx36 in mammalian neurons. *Brain Research Reviews, 32*(1), 72-85.

Cox, D. R., & Lewis, P. A. (1966). *The statistical analysis of series of events*. London: Methuen.

Cullen, K. E. (2004). Sensory signals during active versus passive movement. *Current Opinion in Neurobiology, 14*(6), 698-706.

Cullen, K. E. (2012). The vestibular system: Multimodal integration and encoding of self-motion for motor control. *Trends in Neurosciences*, *35*(3), 185-196.

Cullen, K. E. (2019). Vestibular processing during natural self-motion: Implications for perception and action. *Nature Reviews Neuroscience, 20*(6), 346-363.

Cullen, K. E., & Roy, J. E. (2004). Signal processing in the vestibular system during active versus passive head movements. *Journal of Neurophysiology, 91*(5), 1919-1933.

Cullen, K. E., Brooks, J. X., Jamali, M., Carriot, J., & Massot, C. (2011). Internal models of self-motion: Computations that suppress vestibular reafference in early vestibular processing. *Experimental Brain Research, 210*(3-4), 377-388.

Cullen, K. E., & Brooks, J. X. (2014). Neural correlates of sensory prediction errors in monkeys: Evidence for internal models of voluntary self-motion in the cerebellum. *The Cerebellum*, *14*(1), 31-34.

Cullen, K. E., & Taube, J. S. (2017). Our sense of direction: Progress, controversies and challenges. *Nature Neuroscience, 20*(11), 1465-1473.

Dale, A., & Cullen, K. E. (2013). The nucleus prepositus predominantly outputs eye movement-related information during passive and active self-motion. *Journal of Neurophysiology*, *109*(7), 1900-1911.

Dale, A., & Cullen, K. E. (2015). Local population synchrony and the encoding of eye position in the primate neural integrator. *Journal of Neuroscience, 35*(10), 4287-4295.

Dean, A. (1981). The variability of discharge of simple cells in the cat striate cortex. *Experimental Brain Research, 44*(4).

Eatock, R. A., & Songer, J. E. (2011). Vestibular hair cells and afferents: Two channels for head motion signals. *Annual Review of Neuroscience*, *34*(1), 501-534.

Eatock, R. A., Rüsch, A., Lysakowski, A., & Saeki, M. (1998). Hair cells in mammalian utricles. *Otolaryngology–Head and Neck Surgery, 119*(3), 172-181.

Gabbiani, F., Metzner, W., Wessel, R., & Koch, C. (1996). From stimulus encoding to feature extraction in weakly electric fish. *Nature, 384*(6609), 564-567.

Goldberg, J. M. (2000). Afferent diversity and the organization of central vestibular pathways. *Experimental Brain Research, 130*(3), 277-297.

Goldberg, J. M. (2012). The vestibular system: A sixth sense. *Oxford University Press*.

Goldberg, J. M., Smith, C. E., & Fernandez, C. (1984). Relation between discharge regularity and responses to externally applied galvanic currents in vestibular nerve afferents of the squirrel monkey. *Journal of Neurophysiology, 51*(6), 1236-1256.

Grüsser, O. J., Pause, M., & Schreiter, U. (1990). Vestibular neurones in the parieto-insular cortex of monkeys (Macaca fascicularis): Visual and neck receptor responses. *The Journal of Physiology*, *430*(1), 559-583.

Hennestad, E., Witoelar, A., Chambers, A., & Vervaeke, K. (2021). Mapping vestibular and visual contributions to angular head velocity tuning in the cortex. *bioRxiv.*

Hitier, M., Besnard, S., & Smith, P. F. (2014). Vestibular pathways involved in cognition. *Frontiers in Integrative Neuroscience, 8.*

Holden, A. V. (1976). *Models of the stochastic activity of neurones.* Berlin: Springer.

Ishizuka, N., Sasaki, S., & Mannen, H. (1982). Central course and terminal arborizations of single primary vestibular afferent fibers from the horizontal canal in the cat. *Neuroscience Letters, 33*(2), 135-139.

Jamali, M., Carriot, J., Chacron, M. J., & Cullen, K. E. (2019). Coding strategies in the otolith system differ for translational head motion vs. static orientation relative to gravity. *eLife, 8.*

Jamali, M., Chacron, M. J., & Cullen, K. E. (2016). Self-motion evokes precise spike timing in the primate vestibular system. *Nature Communications, 7*(1).

Lasker, D. M., Han, G. C., Park, H. J., & Minor, L. B. (2008). Rotational responses of vestibular–nerve afferents innervating the semicircular canals in the C57BL/6 mouse. *Journal of the Association for Research in Otolaryngology, 9*(3), 334-348.

Laughlin, S. (1981). A simple coding procedure enhances a Neuron's information capacity. *Zeitschrift für Naturforschung C*, 36(9-10), 910-912.

Liu, S., Gu, Y., DeAngelis, G. C., & Angelaki, D. E. (2013). Choice-related activity and correlated noise in subcortical vestibular neurons. *Nature Neuroscience*, *16*(1), 89-97.

Mackrous, I., Carriot, J., Cullen, K. E., & Chacron, M. J. (2020). Neural variability determines coding strategies for natural self-motion in macaque monkeys. *eLife*, *9*.

Magnin, M., & Fuchs, A. (1977). Discharge properties of neurons in the monkey thalamus tested with angular acceleration, eye movement and visual stimuli. *Experimental Brain Research, 28-28*(3-4).

Mainen, Z., & Sejnowski, T. (1995). Reliability of spike timing in neocortical neurons. *Science, 268*(5216), 1503-1506.

Marlinski, V., & McCrea, R. A. (2009). Self-motion signals in vestibular nuclei neurons projecting to the thalamus in the alert squirrel monkey. *Journal of Neurophysiology*, *101*(4), 1730-1741.

Massot, C., Schneider, A. D., Chacron, M. J., & Cullen, K. E. (2012). The vestibular system implements a linear–nonlinear transformation in order to encode self-motion. *PLoS Biology*, *10*(7), e1001365.

Massot, C., Chacron, M. J., & Cullen, K. E. (2011). Information transmission and detection thresholds in the vestibular nuclei: Single neurons vs. population encoding. *Journal of Neurophysiology*, *105*(4), 1798-1814.

McCrea, R. A., Strassman, A., May, E., & Highstein, S. M. (1987). Anatomical and physiological characteristics of vestibular neurons mediating the horizontal vestibulo-ocular reflex of the squirrel monkey. *The Journal of Comparative Neurology, 264*(4), 547-570.

Medrea, I., & Cullen, K. E. (2013). Multisensory integration in early vestibular processing in mice: The encoding of passive vs. active motion. *Journal of Neurophysiology, 110*(12), 2704-2717.

Metzen, M. G., & Chacron, M. J. (2015). Neural Heterogeneities determine response characteristics to second-, but not first-order stimulus features. *Journal of Neuroscience, 35*(7), 3124-3138.

Mitchell, D. E., Kwan, A., Carriot, J., Chacron, M. J., & Cullen, K. E. (2018). Neuronal variability and tuning are balanced to optimize naturalistic self-motion coding in primate vestibular pathways. *eLife, 7.*

Newlands, S. D., & Perachio, A. A. (2003). Central projections of the vestibular nerve: A review and single fiber study in the mongolian gerbil. *Brain Research Bulletin, 60*(5-6), 475-495.

Payne, H. L., & Raymond, J. L. (2017). Magnetic eye tracking in mice. *eLife, 6.*

Poulet, J. F., & Petersen, C. C. (2008). Internal brain state regulates membrane potential synchrony in barrel cortex of behaving mice. *Nature, 454*(7206), 881-885.

Rieke, F. (1996). *Spikes: Exploring the neural code.* MIT Press.

Roddey, J.C., Girish, B. & Miller, J.P. (2000) Assessing the Performance of Neural Encoding Models in the Presence of Noise. *Journal of Computational Neuroscience, 8,* 95–112 .

Roy, J. E., & Cullen, K. E. (2001). Selective processing of vestibular Reafference during self-generated head motion. *The Journal of Neuroscience, 21*(6), 2131-2142.

Roy, J. E., & Cullen, K. E. (2004). Dissociating self-generated from passively applied head motion: Neural mechanisms in the vestibular nuclei. *Journal of Neuroscience*, *24*(9), 2102-2111.

Sadeghi, S. G., Chacron, M. J., Taylor, M. C., & Cullen, K. E. (2007b). Neural variability, detection thresholds, and information transmission in the vestibular system. *Journal of Neuroscience, 27*(4), 771-781.

Sadeghi, S. G., Minor, L. B., & Cullen, K. E. (2007a). Response of vestibular-nerve afferents to active and passive rotations under normal conditions and after unilateral Labyrinthectomy. *Journal of Neurophysiology*, *97*(2), 1503-1514.

Sato, F., Sasaki, H., Ishizuka, N., Sasaki, S., & Mannen, H. (1989). Morphology of single primary vestibular afferents originating from the horizontal semicircular canal in the cat. *The Journal of Comparative Neurology, 290*(3), 423-439.

Schneider, A. D., Jamali, M., Carriot, J., Chacron, M. J., & Cullen, K. E. (2015). The increased sensitivity of irregular peripheral canal and otolith vestibular afferents optimizes their encoding of natural stimuli. *Journal of Neuroscience, 35*(14), 5522-5536.

Shadlen, M. N., & Newsome, W. T. (1998). The variable discharge of cortical neurons: Implications for connectivity, computation, and information coding. *The Journal of Neuroscience, 18*(10), 3870-3896.

Shadmehr, R., Smith, M. A., & Krakauer, J. W. (2010). Error correction, sensory prediction, and adaptation in motor control. *Annual Review of Neuroscience*, *33*(1), 89-108.

Shinder, M. E., & Taube, J. S. (2010). Differentiating ascending vestibular pathways to the cortex involved in spatial cognition. *Journal of Vestibular Research, 20*(1,2), 3-23.

Simoncelli, E. P., & Olshausen, B. A. (2001). Natural image statistics and neural representation. *Annual Review of Neuroscience, 24*(1), 1193-1216.

Smith, C. E., & Goldberg, J. M. (1986). A stochastic afterhyperpolarization model of repetitive activity in vestibular afferents. *Biological Cybernetics, 54*(1), 41-51.

Softky, W., & Koch, C. (1993). The highly irregular firing of cortical cells is inconsistent with temporal integration of random EPSPs. *The Journal of Neuroscience, 13*(1), 334-350.

Sylvestre, P. A., & Cullen, K. E. (1999). Quantitative analysis of Abducens Neuron discharge dynamics during saccadic and slow eye movements. *Journal of Neurophysiology, 82*(5), 2612-2632.

Theunissen, F., & Miller, J. P. (1995). Temporal encoding in nervous systems: A rigorous definition. *Journal of Computational Neuroscience, 2*(2), 149-162.

Tolhurst, D., Movshon, J., & Dean, A. (1983). The statistical reliability of signals in single neurons in cat and monkey visual cortex. *Vision Research, 23*(8), 775-785.

Uchino, Y., Sasaki, M., Sato, H., Bai, R., & Kawamoto, E. (2005). Otolith and canal integration on single vestibular neurons in cats. *Experimental Brain Research, 164*(3), 271-285.

Yakushin, S. B., Raphan, T., & Cohen, B. (2006). Spatial properties of central vestibular neurons. *Journal of Neurophysiology, 95*(1), 464-478.